OUKA
The University of Osaka
Institutional Knowledge Archive

Title	Dynamic kinetic resolution of tert-alcohols via combination of a lipase/Brønsted acid in a biphasic reaction medium
Author(s)	Kin, Takusho; Horino, Satoshi; Moon, Jihoon et al.
Citation	Green Chemistry. 2025
Version Type	AM
URL	https://hdl.handle.net/11094/102428
rights	Reproduced from Green Chem., 2025 with permission from the Royal Society of Chemistry.
Note	

The University of Osaka Institutional Knowledge Archive : OUKA

https://ir.library.osaka-u.ac.jp/

The University of Osaka

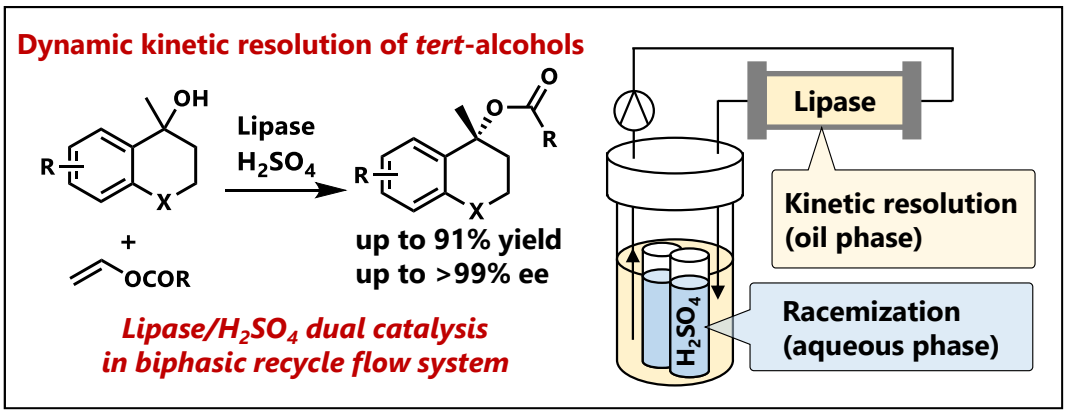
Dynamic Kinetic Resolution of *tert*-Alcohols *via* Combination of Lipase/Brønsted Acid in Biphasic Reaction Medium

Takusho Kin,[a] Satoshi Horino,[a] Jihoon Moon,[a] Momoka Tsuda,[a] Harald Gröger,[a,b] Shuji Akai*[a,†] and Kyohei Kanomata*[a]

a. Graduate School of Pharmaceutical Sciences, The University of Osaka, 1-6 Yamadaoka, Suita, Osaka 565-0871, Japan. Email: kanomata@phs.osaka-u.ac.jp
b. Chair of Industrial Organic Chemistry and Biotechnology, Faculty of Chemistry, Bielefeld University, Universitätsstraße 25, 33615 Bielefeld, Germany.
† Current address: SANKEN, The University of Osaka, 8-1 Mihogaoka, Ibaraki, Osaka 567-0047, Japan

Abstract

Chemoenzymatic dynamic kinetic resolution (DKR) provides a promising green approach for synthesizing optically active alcohols and their derivatives, which serve as widely used key intermediates in the fine chemical industry. While lipase-catalysed DKR of secondary alcohols has been extensively studied, the DKR of tertiary alcohols remains a significant challenge, even in advanced organic synthesis. This is mainly because *tert*-alcohols are poorly reactive to esterification owing to steric hindrance and are prone to dehydrative side reactions. In this study, the combined use of a lipase and the strong Brønsted acid H_2SO_4 enabled the efficient DKR of racemic *tert*-alcohols to produce the corresponding esters with high enantiomeric excess (95–99% ee) in 56–91% isolated yields. In this DKR system, lipase-catalysed kinetic resolution in the oil phase and H_2SO_4-catalysed racemization of the unreacted enantiomer of the alcohol in the aqueous phase proceeded concurrently in one reactor. This simultaneous use of the inherently incompatible combination of lipase and a strong Brønsted acid was realized by integrating phase separation via a hydrophobic polydimethylsiloxane membrane and a recycling flow reaction system. In addition, side reactions were completely suppressed by conducting the racemization reaction in the aqueous phase, enabling the application of this DKR methodology to a range of *tert*-alcohols, thus demonstrating, for the first time, a generally applicable DKR system for *tert*-alcohols.



Introduction

Over the last decade, there has been a significant surge in interest regarding multicatalytic systems, wherein two or more catalysts collaborate synergistically to promote the intricate synthesis of valuable molecules.[1,2] Such multicatalytic systems have facilitated the development of sustainable and economical processes in organic synthesis, notably in the realm of asymmetric transformation.[3–5] The use of enzymes as catalysts in chiral control is particularly attractive due to their renewable nature and substrate specificity, enabling the production of high enantiomeric excess products in an environmentally friendly manner under mild reaction conditions. While sequential combinations of enzymes with chemocatalysts have been widely explored, the integration of these two types of catalysts in one-pot synthesis to develop chemoenzymatic processes has remained largely unexplored because of the inherent challenges of avoiding the mutual deactivation of both catalysts.[6–9]

The dynamic kinetic resolution (DKR) of racemic alcohols is a representative transformation in the field of chemoenzymatic catalysis, wherein lipase-catalysed enantioselective esterification in an organic solvent is coupled with chemocatalytic racemization of the unreacted alcohol enantiomers (Fig. 1a).[10–12] The DKR is particularly attractive in green and sustainable synthesis as it overcomes the intrinsic limitation of kinetic resolution, which restricts the theoretical maximum product yield to 50%. While the chemoenzymatic DKR of *sec*-alcohols has been intensively studied using lipases,[13] the DKR of *tert*-alcohols still remains a formidable challenge, despite the importance of enantiomerically enriched *tert*-alcohols and their derivatives in industry and academic studies.[14–17] Lipase A from *Candida antarctica* (CAL-A) has a unique substrate binding site[18,19] and has been employed in the kinetic resolution of *tert*-alcohols.[20–24] Meanwhile, Lewis-acid or Brønsted-acid catalysts have been used for the racemization of *tert*-alcohols via carbocation intermediates,[25–27] in sharp contrast to *sec*-alcohols, for which redox catalysis via ketone intermediates is also effective (Fig. 1b).[28] The DKR of *tert*-alcohol was reported using a combination of CAL-A with a mesoporous silica-supported oxovanadium as the racemization catalyst (Fig. 1c).[29] However, this DKR was applicable for only one substrate and suffered from long reaction times, insufficient catalyst efficiency, and side reactions. In particular, *tert*-alcohols are prone to dehydrative side reactions that form alkenes under acidic conditions.[26,29] Additionally, lipases are poorly compatible with acid catalysts and lose their catalytic activity during these reactions.

Dehydrative side reactions that occur during acid-catalysed racemization of alcohols are effectively suppressed in aqueous media due to the rapid reaction of carbocation intermediates with water, which regenerates the racemic alcohols.[26,30] Brønsted acid-catalysed racemization in aqueous phase has been incorporated into the DKR of *sec*-alcohols using a biphasic reaction medium within a Pickering emulsion.[30] In this system, lipase-catalysed esterification proceeds in the oil phase, while acid-catalysed racemization occurs in the aqueous phase. However, the direct application of this DKR method to *tert*-alcohols has proven unsuccessful due to their higher susceptibility to dehydrative side reactions and significantly lower reactivity in lipase-catalysed esterification compared to *sec*-alcohols (See page S12 in Supporting Information for the details).[31] In this study, these challenges were successfully overcome through the compartmentalization of the oil/water biphasic medium using a hydrophobic membrane with selective permeability, integrated with a recycling flow system to enhance lipase

catalysis. The present system, for the first time, enables a practical DKR applicable to a range of tertiary alcohols, providing the corresponding esters with high yields and excellent enantiomeric purities (Fig. 1d).[32]

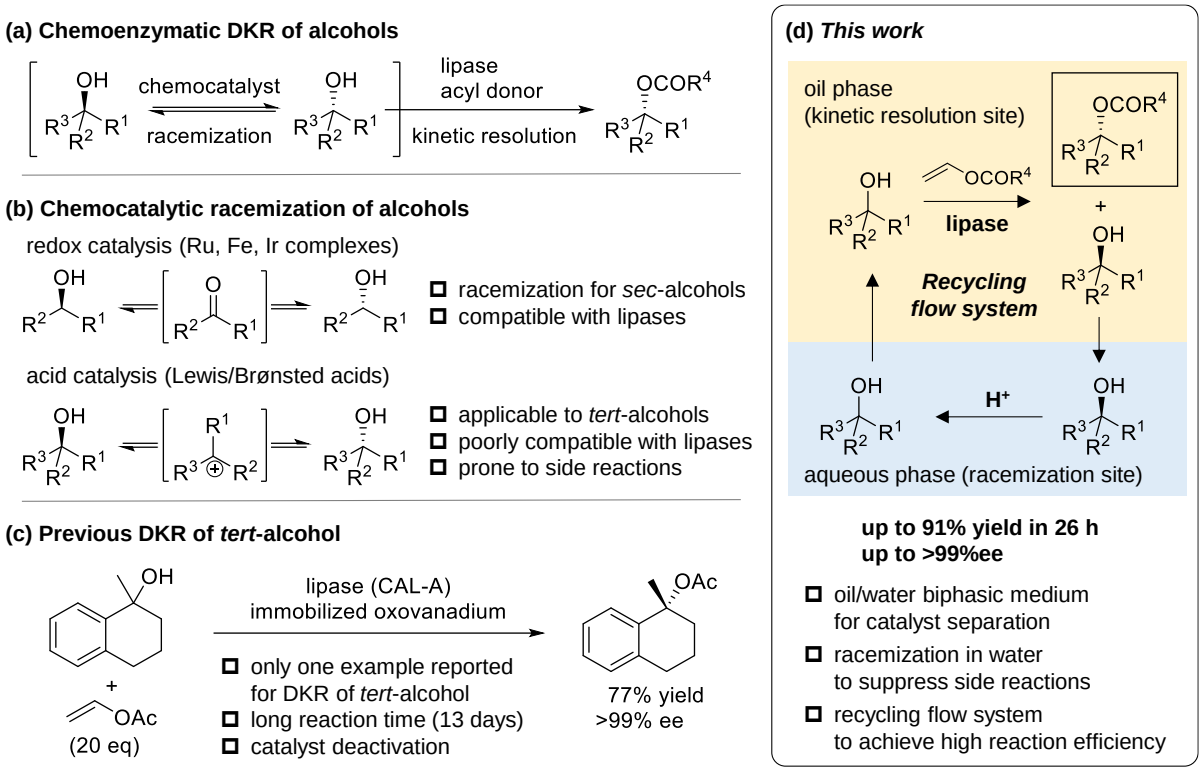


Fig. 1 Dynamic kinetic resolution (DKR) of *tert*-alcohol.

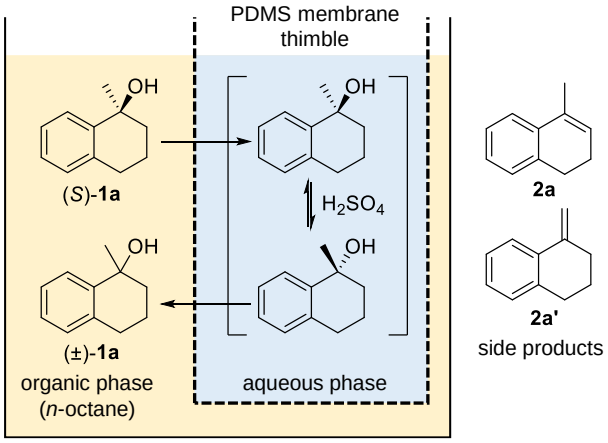
Results and discussion

At the outset of our research, we opted for polydimethylsiloxane (PDMS) membranes to compartmentalize the oil/water biphasic media, thus enabling the simultaneous use of two types of catalysts in a single reaction system. PDMS membranes have selective permeability for small hydrophobic molecules, while water, salts, and high-polarity molecules exhibit minimal flux rates through the membrane.[33–35] In addition, PDMS membranes are advantageous owing to their facile preparation and versatility for molding into the desired shape for the reactors.[34] In this study, PDMS was molded into thimbles that were 5 mm in diameter and 30 mm in length, and an aqueous H_2SO_4 solution was sealed in these thimbles for use as a racemization catalyst (see ESI for details on the preparation of the PDMS thimbles).

The racemization reaction of *tert*-alcohol **1a** was investigated by immersing the H_2SO_4-containing PDMS thimbles in an *n*-octane solution of (*S*)-**1a** (61% ee) at 25 °C (Table 1; see also ESI, Table S1 and Fig. S1). The racemization rate increased with the concentration of H_2SO_4.[30] In particular, the half-life of racemization ($t_{1/2}$) decreased from 12 h to 5 h when the H_2SO_4 concentration was increased from 5 mM to 30 mM (Table 1, entries 1–4). The racemization rate further increased with

increasing number of PDMS thimbles (Table 1, entries 5 and 6). Notably, only trace amounts (<5%) of the side products, namely, the alkenes **2a** and **2a'**, were observed under these conditions, suggesting that acid-catalysed racemization in aqueous media effectively suppressed alkene formation. Thus, a notable advantage of employing an H_2SO_4 solution in PDMS thimbles as the racemization catalyst is the ability to precisely adjust its concentration and volume, thereby allowing for optimizing the racemization rate while minimizing side reactions.

Table 1. H_2SO_4-catalysed racemization of **1a** in compartmentalized oil/water biphasic solution[a]

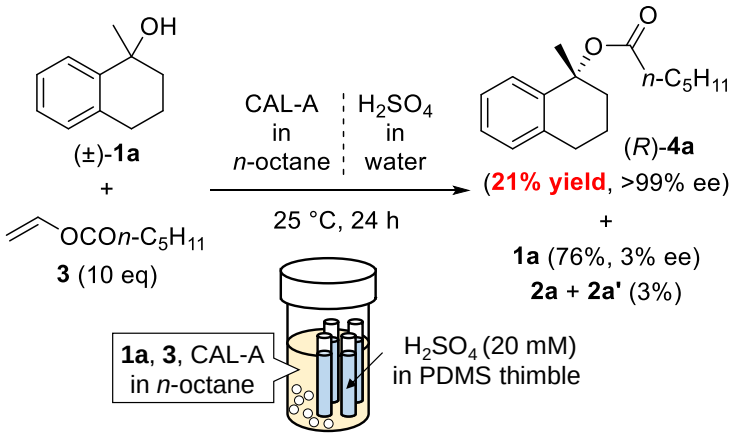


Entry	H_2SO_4 (mM)	Number of thimbles	$t_{1/2}$ (h)	%Recovery of **1a** (**2a**+**2a'**)[b]
1	5	2	12.4	>95 (n.d.)
2	10	2	9.8	>95 (n.d.)
3	20	2	8.3	>95 (2)
4	30	2	5.0	>95 (4)
5	20	3	5.3	>95 (3)
6	20	4	3.6	95 (5)

[a] Unless otherwise noted, the reaction was conducted using (*S*)-**1a** (61% ee, 0.15 mmol) and *n*-octane (3.0 mL) at 25 °C in a ø27 mm vial. Each PDMS thimble contained 0.3 mL of aq. H_2SO_4. [b] Quantified after 24 h of reaction by ^{1}H NMR analysis using an internal standard. The total yields of **2a** and **2a'** are in the parentheses. n.d.: not detected.

After establishing the racemization conditions using aqueous H_2SO_4 in PDMS thimbles, we next investigated the DKR of *tert*-alcohols by combining the racemization process with acylative kinetic resolution using a commercial CAL-A (recombinant enzyme immobilized on methacrylate polymer).[23] The reaction was conducted by immersing the PDMS thimbles containing aqueous H_2SO_4 (20 mM) in an *n*-octane solution of (±)-**1a** and vinyl hexanoate (**3**) containing CAL-A (Scheme 1).[23] However, the

DKR afforded the corresponding ester **4a** in only 21% yield after reacting for 24 h at 25 °C, along with 76% of **1a** and 3% of the alkenes **2a** and **2a'**. Despite intensive screening of the reaction conditions, no significant increase in the product yield was achieved. Meanwhile, the complete consumption of 10 equiv of **3** was observed in all trials, indicating that the hydrolysis of **3** competed with the esterification of **1a** in biphasic DKR. In addition, the deactivation of lipase CAL-A was observed during the reaction; adding another portion of **3** during the reaction did not increase the conversion of **1a**. Despite these limitations, the DKR methodology utilizing aqueous acid racemization remained promising because the racemization proceeded smoothly (3% ee for recovered **1a**) while a high mass balance of **1a** and **4a** was maintained (>90%) without significant side reactions.



Scheme 1. Lipase/H_2SO_4-cocatalysed DKR of **1a** in a biphasic medium. The reaction was conducted using (±)-**1a** (0.15 mmol), **3** (1.5 mmol), CAL-A (50 mg), and PDMS thimbles (×4, each containing 0.3 mL of 20 mM H_2SO_4) in *n*-octane (3 mL) at 25 °C in a ø27 mm vial.

When gaining further insight into this process, the low efficiency of the abovementioned DKR methodology was attributed to the lipase-catalysed kinetic resolution process, as the conversion did not improve even with a prolonged reaction time. To address this issue, we employed a flow reaction in a column reactor packed with lipase; we expected that the passing of the reactant solution through a column containing a sufficient amount of lipase would significantly enhance the esterification process while minimizing undesired hydrolysis by reducing the contact time between the lipase and **3** and **4a**.

During the initial screening of suitable flow reaction conditions, we found that mixing Celite with immobilized CAL-A to modulate the residence time was effective in enhancing the conversion (Supporting Information, Fig. S2).[36] Then, we investigated the effects of additives to enhance the conversion of kinetic resolution under flow conditions (Fig. 2, see also Figs. S3 and S4); the conversion decreased significantly after 1 h of operation without any additives (empty circles). This decline in conversion was likely due to the deactivation of the acid-labile lipase by hexanoic acid, a side product generated by the hydrolysis of **3**. Our previous studies demonstrated the positive effects of inorganic base additives on lipase-catalysed esterification and the DKR.[23,37–39] Consequently, we mixed Na_2CO_3

with CAL-A and Celite to pack the reactor, which significantly improved the conversion and lipase stability over extended periods of time (filled circles). After 6 h of operation, 73% of the initial activity was maintained in the presence of Na_2CO_3, whereas the activity decreased to 54% of the initial activity in its absence. Notably, this flow kinetic resolution achieved >20% conversion in a short residence time (20 min), suggesting that the reaction rate was significantly improved compared to batch conditions.

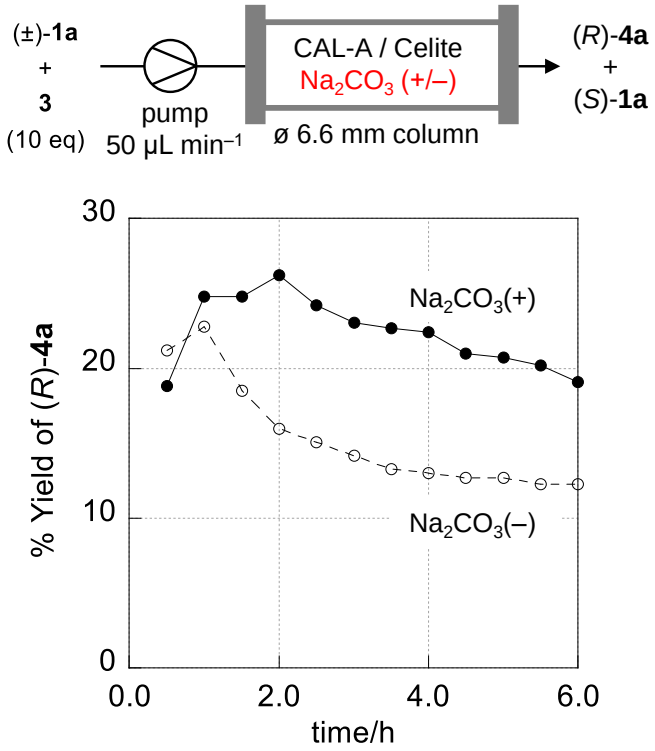


Fig. 2. Kinetic resolution of (±)-**1a** under flow conditions. An *n*-octane solution containing (±)-**1a** (0.05 M) and **3** (0.5 M) was flowed at a rate of 50 μL min^{-1} (residence time 20 min); (○) CAL-A (50 mg) and Celite (550 mg) were packed in the reactor (35 mm length); (●) CAL-A (50 mg), Celite (450 mg), and Na_2CO_3 (300 mg) were packed in the reactor (35 mm length).

With flow kinetic resolution successfully achieved, we combined it with H_2SO_4-catalysed racemization to investigate the DKR of (±)-**1a**. A recycling flow system[40] was constructed to circulate the organic phase between the flow reactor and the vial in which racemization was conducted, enabling the DKR process through repeated kinetic resolution and racemization cycles (Fig. 3; see also Fig. S5 in Supporting Information for the photograph of the reaction setup). The kinetic resolution of (±)-**1a** with **3** to afford (*R*)-**4a** was proceeded in a column reactor containing CAL-A, and the racemization of unreacted (*S*)-**1a** occurred in a vial wherein sealed PDMS thimbles containing an aqueous H_2SO_4 solution were immersed in *n*-octane. Magnesium sulfate was packed at the reactor inlet to remove trace amounts of water that permeated from the PDMS thimbles. When (±)-**1a** was reacted under the recycling flow conditions, (*R*)-**4a** was obtained in 91% isolated yield with >99% ee after 24 h.

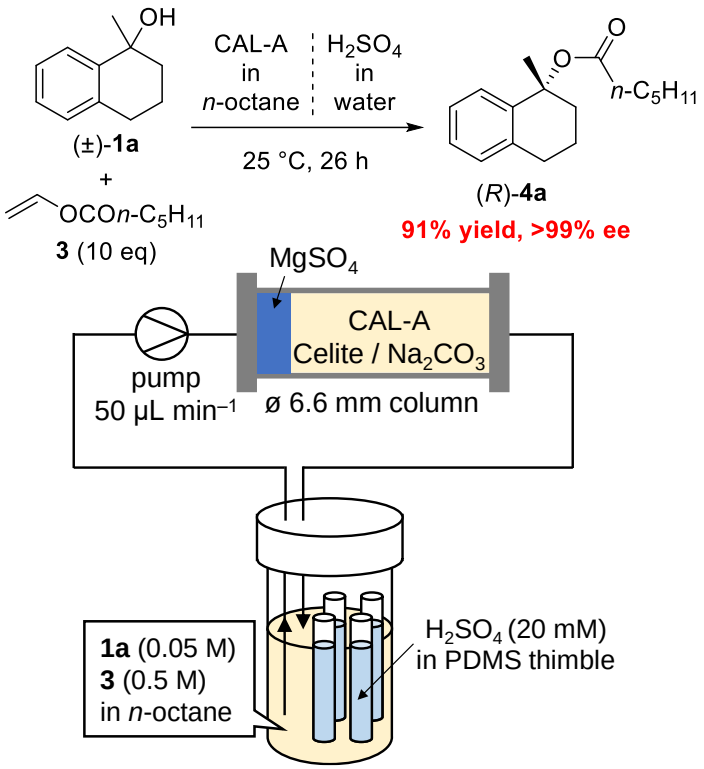
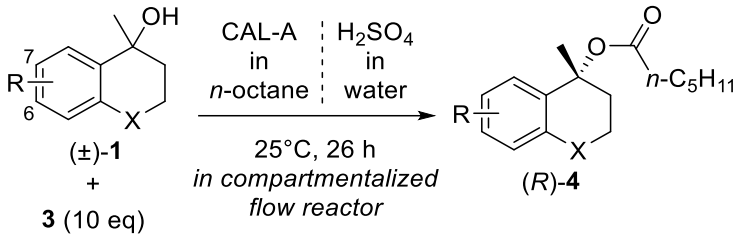


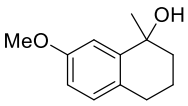
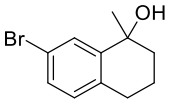
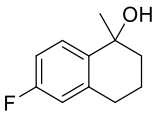
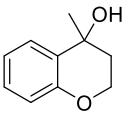
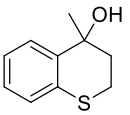
Fig. 3. CAL-A/H_2SO_4-cocatalysed DKR of (±)-**1a** in compartmentalized recycling flow reactor. The reaction was conducted using (±)-**1a** (0.15 mmol), **3** (1.5 mmol), CAL-A (50 mg), Celite (330 mg), Na_2CO_3 (200 mg), $MgSO_4$ (140 mg), PDMS thimbles (×4, each containing 0.3 mL of 20 mM H_2SO_4), and *n*-octane (3.3 mL), and the organic solution was circulated at a flow rate of 50 µL min^{-1} for 26 h at 25 °C. See Supporting Information for the detailed experimental procedure and photograph of the reaction setup.

The substrate scope of the DKR method was investigated using the optimal reaction conditions obtained for the established flow system. Based on our recent study on the lipase-catalysed kinetic resolution of *tert*-alcohols, tetralin derivatives **1b**–**1f** were employed as substrates (Table 2).[23] Fine-tuning of the H_2SO_4 concentration for each substrate enabled optimization of the racemization rate and minimization of the side reactions, leading to the successful DKR of these compounds (Supporting Information, Table S2). The DKR of 7-MeO-substituted **1b** and 6-F-substituted **1d** proceeded smoothly with 25–30 mM aq. H_2SO_4, and the corresponding esters (*R*)-**4b** and (*R*)-**4d** were obtained in 87% and 83% yields, respectively, both with high enantiomeric excess (>98% ee; Table 2, Entries 1 and 3). Meanwhile, the DKR of **1c** bearing a 7-Br-substituent required a much higher H_2SO_4 concentration because racemization was considerably slower than for **1b** and **1d**. Accordingly, the reaction resulted in a moderate yield (56%) of (*R*)-**4c** using 2.5 M H_2SO_4 and 20% recovery of **1c** (33% ee); however, the enantiomeric excess of (*R*)-**4c** was high (>99% ee; Table 2, Entry 2). Alcohols **1e** and **1f**, in which the C4 carbon was replaced by oxygen and sulfur, respectively, were also subjected to the present DKR method, affording **4e** (80%, 96% ee; Table 2, Entry 4) and **4f** (78%, 98% ee; Table 2, Entry 5), respectively. Toluene was used as the co-solvent because of the low solubility of (±)-**1e** and (±)-**1f** in *n*-

octane. The slightly lower enantiomeric excess of **4e** (96% ee) was attributed to the inherent selectivity of lipase in the kinetic resolution of **1e**.[23] Notably, this chemoenzymatic DKR allows the successful conversion of a range of *tert*-alcohols, leading to the desired esters in high yield and enantioselectivity, which is in contrast to our previous method being suitable only for one example.[29]

Table 2. Substrate scope of the flow DKR method[a]



Entry	**1**		H_2SO_4 (mM)	(*R*)-**4**	% Conversion[b]	% Yield[c]	% ee[d]
1		**1b**	25	**4b**	89	87	>99
2		**1c**	2.5×10^3	**4c**	80[e]	56	>99
3		**1d**	30	**4d**	84	83	>99
4[f,g]		**1e**	25	**4e**	83	80	96
5[f,g]		**1f**	70	**4f**	80	78	98

[a] Unless otherwise noted, the reaction was conducted using (±)-**1a** (0.15 mmol) and **3** (1.5 mmol). CAL-A (50 mg) and PDMS thimbles (×4, each containing 0.3 mL of H_2SO_4) were used and *n*-octane (3.3 mL) was circulated for 26 h at 25 °C. See Supporting Information for the detailed experimental procedure. [b] Determined based on the amount of recovered **1** after the reaction. [c] Isolated yield. [d] Determined by chiral HPLC analysis. [e] Alkene **2c** (21%) was formed. [f] The reaction was conducted in *n*-octane/toluene (3:1 v/v) for 46 h. [g] Additional 10 eq of **3** was added at 24 h.

Conclusions

We developed the first generally applicable system for the DKR of *tert*-alcohols using lipase/H_2SO_4-cocatalysis. A compartmentalized reaction medium combined with a recycling flow system was essential to realize dual catalysis; in our system, compartmentalization of the oil and aqueous phases was achieved using a semipermeable PDMS membrane selective for small hydrophobic molecules. The efficiency of the lipase-catalysed kinetic resolution was significantly enhanced when the process was conducted in a flow system with Na_2CO_3 as an additional component in the packed bed reactor. Notably, the DKR was applied to a range of *tert*-alcohols by fine-tuning the H_2SO_4 concentration for each substrate to suppress dehydrative side reactions. The DKR of *tert*-alcohols incorporating catalytic racemization has been reported for only one compound to date.[29] The biphasic flow DKR system described in this study is the first general and practical DKR method applicable to various *tert*-alcohols. Although the substrate scope is currently limited to cyclic *tert*-alcohols due to the substrate spectrum of the wild-type CAL-A, further expansion of the scope is under investigation using the engineered CAL-A variant we reported recently.[24] Applications of this biphasic flow system for a variety of dual catalysts are also currently ongoing in our laboratory.

Author contributions

K.K. and S.A. conceived and supervised the project. T. K. conducted all the experiments in this manuscript. J. M. and T. K. conducted the initial assessment of the biphasic reaction system for this project. M. T. conducted experiments required in the revision process. S. H. and H. G. guided the preparation and use of PDMS membrane. T. K. and K. K. are responsible for all the data analysis. K. K., T. K., and S. A. wrote the manuscript. All authors have given approval to the final version of the manuscript.

Conflicts of interest

There are no conflicts to declare.

Acknowledgements

We would like to appreciate Dr. Koichiro Masuda (National Institute of Advanced Industrial Science and Technology (AIST), Japan) for fruitful discussion regarding flow reaction and Mr. Yasuo Nakanishi (Garret Labo, Osaka, Japan) for technical support on the recycling flow system. This work was financially supported by the JSPS KAKENHI (Grant Numbers 24K08410 (K.K.) and 24K02148 (S.A.)), The Research Foundation for Pharmaceutical Sciences (K.K.), Nissan Chemical Research Planning Award from the Society of Synthetic Organic Chemistry, Japan (K.K.), Tokuyama Science Foundation (K.K.), Japan Foundation for Applied Enzymology (K.K.), Amano Institute of Technology (K.K.), the Joint Usage/Research Center for Catalysis (23AY0215, 24AY0545) (K.K.), “Innovation inspired by

Nature" Research Support Program, SEKISUI CHEMICAL CO., LTD. (K.K.), the Platform Project for Supporting Drug Discovery and Life Science Research (Basis for Supporting Innovative Drug Discovery and Life Science Research (BINDS)) from AMED (Grant Number 24ama121054), and the Deutsche Forschungsgemeinschaft (DFG; Grant number: GR 3461/7-1). In addition, H.G. thanks The University of Osaka for a "Specially Appointed Professorship" at the Graduate School of Pharmaceutical Sciences of The University of Osaka.

Notes and references

1 T. L. Lohr and T. J. Marks, *Nat. Chem.*, 2015, **7**, 477–482.
2 S. Martínez, L. Veth, B. Lainer and P. Dydio, *ACS Catal.*, 2021, **11**, 3891–3915.
3 X. Xiao, B. X. Shao, Y. J. Lu, Q. Q. Cao, C. N. Xia and F. E. Chen, *Adv. Synth. Catal.*, 2021, **363**, 352–387.
4 H. Sun, Y. Ma, G. Xiao and D. Kong, *Trends Chem.*, 2024, **14**, 3812–3844.
5 G. L. Thejashree, E. Doris, E. Gravel and I. N. N. Namboothiri, *Eur. J. Org. Chem.*, 2022, **2022**, e202201035.
6 H. Gröger and K. Zelenska, in *Comprehensive Chirality*, Academic Press, 2024, pp. 361–388.
7 H. Gröger, F. Gallou and B. H. Lipshutz, *Chem. Rev.*, 2023, **123**, 5262–5296.
8 S. González-Granda, L. Escot, I. Lavandera and V. Gotor-Fernández, *Angew. Chem. Int. Ed.*, 2023, **62**, e202217713.
9 S. González-Granda, J. Albarrán-Velo, I. Lavandera and V. Gotor-Fernández, *Chem. Rev.*, 2023, **123**, 5297–5346.
10 O. Verho and J. E. Bäckvall, *J. Am. Chem. Soc.*, 2015, **137**, 3996–4009.
11 L. C. Yang, H. Deng and H. Renata, *Org. Process Res. Dev.*, 2022, **26**, 1925–1943.
12 J. E. Bäckvall, Ed., *Dynamic Kinetic Resolution (DKR) and Dynamic Kinetic Asymmetric Transformations (DYKAT)*, Thieme: Stuttgart, 2023.
13 K. Kanomata and S. Akai, in *Science of Synthesis: Dynamic Kinetic Resolution (DKR) and Dynamic Kinetic Asymmetric Transformations (DYKAT)*, ed. J. E. Bäckvall, Thieme: Stuttgart, 2023, pp. 181–217.
14 O. Riant and J. Hannedouche, *Org. Biomol. Chem.*, 2007, **5**, 873–888.
15 M. Müller, *ChemBioEng Rev.*, 2014, **1**, 14–26.
16 Y. L. Liu and X. T. Lin, *Adv. Synth. Catal.*, 2019, **361**, 876–918.
17 Y. P. He, D. Tian, X. Z. Li and H. Wu, *Org. Chem. Front.*, 2023, **10**, 3110–3129.
18 D. J. Ericsson, A. Kasrayan, P. Johansson, T. Bergfors, A. G. Sandström, J. E. Bäckvall and S. L. Mowbray, *J. Mol. Biol.*, 2008, **376**, 109–119.
19 R. R. C. Monteiro, J. J. Virgen-Ortiz, Á. Berenguer-Murcia, T. N. da Rocha, J. C. S. dos Santos, A. R. Alcántara and R. Fernandez-Lafuente, *Catal. Today*, 2021, **362**, 141–154.
20 S. Hari Krishna, M. Persson and U. T. Bornscheuer, *Tetrahedron: Asymmetry*, 2002, **13**, 2693–2696.
21 J. Löfgren, T. Görbe, M. Oschmann, M. Svedendahl Humble and J. E. Bäckvall, *ChemBioChem*,

2019, **20**, 1438–1443.
22 L. G. Neto, C. D. F. Milagre and H. M. S. Milagre, *Results Chem.*, 2023, **5**, 100966.
23 S. Horino, K. Wagner, A. Hummel, K. Kanomata, H. Gröger and S. Akai, *Eur. J. Org. Chem.*, 2024, **27**, e202400242.
24 K. Wagner, A. Hummel, J. Yang, S. Horino, K. Kanomata, S. Akai and H. Gröger, *ChemBioChem*, 2024, **25**, e202400082.
25 H. Gröger, S. Horino, K. Kanomata and S. Akai, *Chem. Eur. J.*, 2024, **30**, e202304028.
26 T. Görbe, R. Lihammar and J. E. Bäckvall, *Chem. Eur. J.*, 2018, **24**, 77–80.
27 G. R. Boyce, S. F. Musolino, J. Yang, A. D. Smith and J. E. Taylor, *J. Org. Chem.*, 2022, **87**, 13367–13374.
28 M. C. Warner and J. E. Bäckvall, *Acc. Chem. Res.*, 2013, **46**, 2545–2555.
29 F. Kühn, S. Katsuragi, Y. Oki, C. Scholz, S. Akai and H. Gröger, *Chem. Commun.*, 2020, **56**, 2885–2888.
30 J. Moon, T. Kin, K. Mizuno, S. Akai and K. Kanomata, *ChemCatChem*, 2023, **15**, e202300878.
31 We are conducting several improvement studies on the lipase-catalysed DKR of *tert*-alcohols in parallel: K. Wagner, S. Horino, A. Hummel, K. Kanomata, S. Akai and H. Gröger, *Chem. Pharm. Bull.*, 2025, **73**, 511–514.
32 The DKR reactions of tetra-substituted hemiacetals and hemiaminals have been reported in which organocatalytic kinetic resolution was coupled with non-catalytic, spontaneous racemization of the substrates: (a) Y. Liu, P. K. Majhi, R. Song, C. Mou, L. Hao, H. Chai, Z. Jin and Y. R. Chi, *Angew. Chem. Int. Ed.*, 2020, **59**, 3859–3863; (b) Y. Y. Gao, C. L. Zhang, L. Dai, Y. F. Han and S. Ye, *Org. Lett.*, 2021, **23**, 1361–1366; (c) H. Zhu, A. Manchado, A. Omar Farah, A. P. McKay, D. B. Cordes, P. H. Y. Cheong, K. Kasten and A. D. Smith, *Angew. Chem. Int. Ed.*, 2024, **63**, e202402908; (d) S. K. Agrawal, P. K. Majhi, A. S. Goodfellow, R. K. Tak, D. B. Cordes, A. P. McKay, K. Kasten, M. Bühl and A. D. Smith, *Angew. Chem. Int. Ed.*, 2024, **63**, e202402909; (e) M. Shan, Y. Yu, M. Sun, S. Yang, M. Wang, B. Zhu and J. Chang, *Chin. Chem. Lett.*, 2025, **36**, 109781.
33 M. B. Runge, M. T. Mwangi, A. L. Miller, M. Perring and N. B. Bowden, *Angew. Chem. Int. Ed.*, 2008, **47**, 935–939.
34 H. Sato, W. Hummel and H. Gröger, *Angew. Chem. Int. Ed.*, 2015, **54**, 4488–4492.
35 J. Hou, S. Chevallier-Michaud, M. Jean, L. Favre, D. Hérault and C. Bressy, *J. Am. Chem. Soc.*, 2023, **145**, 27236–27241.
36 R. Ikeda, T. Nishio, K. Kanomata and S. Akai, *Chem. Pharm. Bull.*, 2024, **72**, 213–219.
37 G. A. I. Moustafa, Y. Oki and S. Akai, *Angew. Chem. Int. Ed.*, 2018, **57**, 10278–10282.
38 G. A. I. Moustafa, K. Kasama, K. Higashio and S. Akai, *RSC Adv.*, 2019, **9**, 1165–1175.
39 K. Kasama, H. Aoyama and S. Akai, *Eur. J. Org. Chem.*, 2020, **2020**, 654–661.
40 (a) P. Ödman, L. A. Wessjohann and U. T. Bornscheuer, *J. Org. Chem.*, 2005, **70**, 9551–9555; (b) M. J. Takle, B. J. Deadman, K. Hellgardt, J. Dickhaut, A. Wieja and K. K. M. Hii, *ACS Catal.*, 2023, **13**, 10541–10546; (c) C. P. Lin, C. H. Xu, F. Y. Meng, S. P. Song, Z. M. Wu, R. C. Zheng and Y. G. Zheng, *Org. Process Res. Dev.*, 2024, **28**, 1886–1895.

Supporting Information

Dynamic Kinetic Resolution of *tert*-Alcohols *via* Combination of Lipase/Brønsted Acid in Biphasic Reaction Medium

Takusho Kin,[a] Satoshi Horino,[a] Jihoon Moon,[a] Momoka Tsuda,[a] Harald Gröger,[a,b] Shuji Akai*[a,‡] and Kyohei Kanomata*[a]

[a]Graduate School of Pharmaceutical Sciences, The University of Osaka, 1-6 Yamadaoka, Suita, Osaka 565-0871, Japan. Email: kanomata@phs.osaka-u.ac.jp

[b]Chair of Industrial Organic Chemistry and Biotechnology, Faculty of Chemistry, Bielefeld University, Universitätsstraße 25, 33615 Bielefeld, Germany.

‡Current address: SANKEN, The University of Osaka, 8-1 Mihogaoka, Ibaraki, Osaka 567-0047, Japan

Table of contents

1. General information 2
2. Preparation of PDMS thimble 2
3. Synthesis of *tert*-alcohols 3
4. H_2SO_4-catalysed racemization of (±)-1 in biphasic medium 5
5. CAL-A-catalysed kinetic resolution of 1a in flow reactor 8
6. Lipase/H_2SO_4-cocatalysed biphasic DKR of (±)-1 11
7. References 14
8. NMR and chiral HPLC chart of product 16

1. General information

All reactions were monitored by thin-layer chromatography (TLC) on glass-backed silica gel 60 F_{254}, 0.2 mm plates (Merck). ^{1}H and ^{13}C NMR spectra were measured on a JEOL JNM-ECA500 (^{1}H: 500 MHz, ^{13}C: 126 MHz, ^{19}F: 471 MHz) instrument. Chemical shifts were reported in δ (ppm) relative to the deuterated solvents (7.26 ppm (^{1}H) and 77.0 ppm (^{13}C) for $CDCl_3$). Data are reported as follows: chemical shift, multiplicity (s = singlet, d = doublet, t = triplet, q = quartet, m = multiplet, br = broad), coupling constants (Hz) and integration. Optical rotation was measured on a JASCO P-1020 polarimeter. All reagents and solvents were purchased from Tokyo Chemical Industry Co., Ltd. (Tokyo, Japan), Nacalai TesqueInc. (Kyoto, Japan), Sigma-Aldrich Co., LLC (Tokyo, Japan), and FUJIFILM Wako Pure Chemical Co., Ltd. (Tokyo, Japan), Kanto Chemical Co., Inc. (Tokyo, Japan), and Kishida Chemical Co., Ltd. (Osaka, Japan), and used without further purification. Unless otherwise noted, flash chromatography was performed on silica gel 60N (particle size 40–50 μm) purchased from Kanto Chemical Co., Inc. Esters **4a**–**4f** were purified by flash chromatography using silica gel modified with aminopropyl groups (Wakogel® 50NH2, FUJIFILM Wako Pure Chemical, Tokyo, Japan). SYLGARD 184 silicone elastomer kit (Dow silicone corporation) was purchased from Amazon Japan Co., Ltd. Mesoporous silica (TMPS-4R) was purchased from Taiyo Kagaku Co., Ltd. (Tokyo, Japan).

In all experiments, immobilized *Candida antarctica* lipase A (CAL-A) purchased from Sigma-Aldrich Co., LLC (Tokyo, Japan) was used as received. Product name: Lipase A *Candida antarctica* immobilized on Immobead 150, recombinant from *Aspergillus oryzae*. Product code: 41658, Lot #: BCCC9785 (activity: 1410 U/g) and BCCF4348 (activity: 1340 U/g)

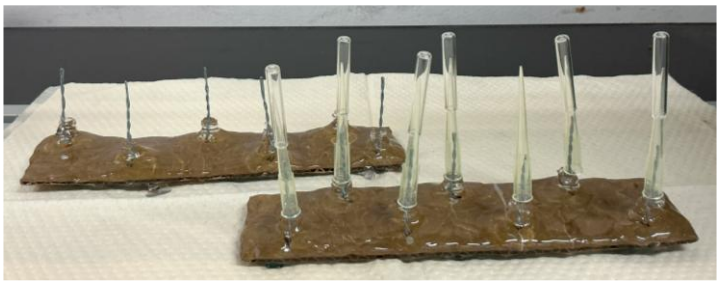
2. Preparation of PDMS thimble

The PDMS thimbles were prepared using SYLGARD 184 silicone elastomer kit according to the reported method with a slight modification.[1,2]

1. **Mixing elastomer**: The elastomer base (10 mL) was mixed with curing agent (1 mL) using a spatula. The mixture was left to stand at 4 °C for 2 h to allow for degassing.
2. **Coating glass inserts**: Glass inserts (4.7 × 30 mm insert for HPLC vial) were attached on a micropipette tip and dipped in the degassed elastomer mixture.



3. **Curing**: The coated glass inserts were mounted on a hand-made wire stand and incubated at 60 °C for 1 h. This coating process was repeated once, followed by overnight incubation at 60 °C to ensure complete curing.



4. **Insert removal**: The coated inserts were soaked in hexane for 2 min to aid in removing the cured PDMS layer from the glass. The resulting PDMS thimbles were then air-dried under ambient conditions.

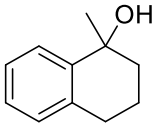




5. **Adding H_2SO_4**: A 300-μL portion of the H_2SO_4 solution was added into each PDMS thimble.
6. **Sealing**: The top edge of each thimble was coated with the elastomer mixture from Step 1. The edge was then sealed by applying heat for 30 sec at 240 °C using a curling iron.

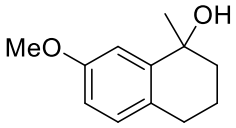
3. Synthesis of *tert*-alcohols

tert-Alcohols (±)-**1a**–**1f** were synthesized according to the reported method.[3,4] Their ^{1}H and ^{13}C NMR spectra were in good agreement with those reported.[4]



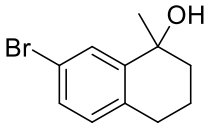
(±)-1-Methyl-1,2,3,4-tetrahydronaphthalen-1-ol (1a)

^{1}H NMR (500 MHz, $CDCl_3$) δ 7.59 (dd, J = 7.5, 1.5 Hz, 1H), 7.23-7.20 (m, 1H), 7.17 (td, J = 7.5, 1.5 Hz, 1H), 7.07 (dd, J = 7.5, 0.9 Hz, 1H), 2.85-2.73 (m, 2H), 1.99-1.89 (m, 3H), 1.87-1.78 (m, 1H), 1.57 (s, 3H); ^{13}C NMR (126 MHz, $CDCl_3$) δ 142.8, 136.2, 128.8, 127.1, 126.34, 126.27, 70.6, 39.8, 30.7, 29.9, 20.4.



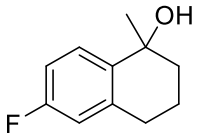
(±)-7-Methoxy-1-methyl-1,2,3,4-tetrahydronaphthalen-1-ol (1b)

^{1}H NMR (500 MHz, $CDCl_3$) δ 7.13 (d, *J* = 2.8 Hz, 1H), 6.99 (d, *J* = 8.4 Hz, 1H), 6.75 (dd, *J* = 8.4, 2.8 Hz, 1H), 3.80 (s, 3H), 2.78-2.66 (m, 2H), 1.98-1.87 (m, 3H), 1.85-1.76 (m, 1H), 1.55 (s, 3H); ^{13}C NMR (126 MHz, $CDCl_3$) δ 158.1, 143.9, 129.8, 128.3, 113.7, 110.7, 70.9, 55.3, 39.8, 30.7, 29.0, 20.6.



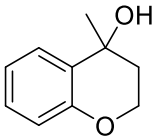
(±)-7-Bromo-1-methyl-1,2,3,4-tetrahydronaphthalen-1-ol (1c)

^{1}H NMR (500 MHz, $CDCl_3$) δ 7.72 (d, *J* = 2.1 Hz, 1H), 7.28 (dd, *J* = 8.2, 2.1 Hz, 1H), 6.94 (d, *J* = 8.2 Hz, 1H), 2.79-2.64 (m, 2H), 1.99-1.85 (m, 3H), 1.84-1.76 (m, 1H), 1.54 (s, 3H); ^{13}C NMR (126 MHz, $CDCl_3$) δ 145.0, 135.0, 130.5, 130.1, 129.4, 119.8, 70.5, 39.4, 30.8, 29.3, 20.2.



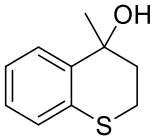
(±)-6-Fluoro-1-methyl-1,2,3,4-tetrahydronaphthalen-1-ol (1d)

^{1}H NMR (500 MHz, $CDCl_3$) δ 7.55 (dd, *J* = 9.0, 6.0 Hz, 1H), 6.90 (td, *J* = 9.0, 2.8 Hz, 1H), 6.75 (dd, *J* = 9.0, 2.8 Hz, 1H), 2.83-2.71 (m, 2H), 1.98-1.87 (m, 3H), 1.86-1.77 (m, 1H), 1.54 (s, 3H); ^{13}C NMR (126 MHz, $CDCl_3$) δ 161.6 (d, $J_{C\text{-}F}$ = 246.6 Hz), 138.63 (d, $J_{C\text{-}F}$ = 7.2 Hz), 138.60 (d, $J_{C\text{-}F}$ = 2.4 Hz), 128.2 (d, $J_{C\text{-}F}$ = 8.4 Hz), 114.7 (d, $J_{C\text{-}F}$ = 20.4 Hz), 113.4 (d, $J_{C\text{-}F}$ = 21.3 Hz), 70.3, 39.7, 30.8, 30.0, 20.3; ^{19}F NMR (471 MHz, $CDCl_3$) δ −116.0 (td, *J* = 9.0, 6.0 Hz, 1F).



(±)-4-Methylchroman-4-ol (1e)

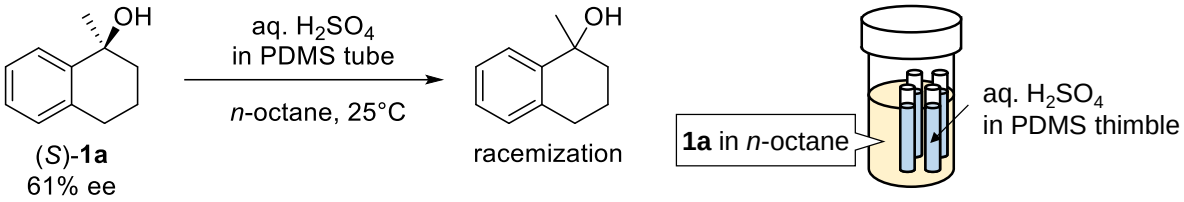
^{1}H NMR (500 MHz, $CDCl_3$) δ 7.49 (dd, *J* = 7.7, 1.6 Hz, 1H), 7.20-1.16 (m, 1H), 6.94 (td, *J* = 7.7, 1.1 Hz, 1H), 6.82 (dd, *J* = 8.2, 1.1 Hz, 1H), 4.29 (ddd, *J* = 11.5, 7.3, 4.2 Hz, 1H), 4.23 (ddd, *J* = 11.5, 5.6, 4.2 Hz, 1H), 2.12-2.04 (m, 2H), 1.64 (s, 3H); ^{13}C NMR (126 MHz, $CDCl_3$) δ 153.8, 129.2, 128.4, 126.4, 120.8, 117.1, 66.4, 63.3, 38.0, 29.5.



(±)-4-Methylthiochroman-4-ol (1f)

^{1}H NMR (500 MHz, $CDCl_3$) δ 7.65-7.63 (m, 1H), 7.13-7.07 (m, 3H), 3.14-3.03 (m, 2H), 2.25-2.17 (m, 2H), 1.58 (s, 3H); ^{13}C NMR (126 MHz, $CDCl_3$) δ 139.6, 132.3, 127.6, 126.4, 126.2, 124.5, 69.3, 38.1, 29.6, 23.5.

4. H_2SO_4-catalysed racemization of (±)-1 in biphasic medium



Typical procedure (Scheme S1): Optically active (*S*)-**1a** was prepared by CAL-A-catalysed kinetic resolution of (±)-**1a** using vinyl hexanoate (**3**) according to our previous report.[4] A solution of (*S*)-**1a** (0.15 mmol, 61% ee) in *n*-octane (3 mL) was added to a 20-mL screw-capped vial (diameter: 27 mm). PDMS thimbles containing aq. H_2SO_4 (300 μL per thimble) were immersed in this solution. The vial was maintained at 25°C in a heating chamber (SLC-25A, Mitsubishi Electric Engineering Ltd., Tokyo, Japan) with gentle stirring of the organic phase. At specified intervals, aliquots of the organic phase were taken for chiral HPLC analysis (Table S1). The rate constant of racemization (k_{rac}) and half-life of % ee ($t_{1/2}$) were calculated from the slop of the ln(%ee) vs time plots.[5] After 24 h, the aqueous phase was neutralized with aq. $NaHCO_3$, combined with the organic phase, and extracted with EtOAc (×3). The combined organic layers were concentrated under reduced pressure, and the residue was analyzed by ^{1}H NMR using 1,4-dimethoxybenzene as the internal standard.

Table S1. Time course of % ee in H_2SO_4-catalysed biphasic racemization of **1a**

Entry	H_2SO_4	number of PMDS thimble		2.0 h	4.5 h	6.0 h	k_{rac} / h^{-1}	$t_{1/2}$ / h
1	5mM	2	%ee	56.9	46.4	43.7		
			ln(%ee)	4.04	3.84	3.78	0.056	12.4
2	10mM	2	%ee	53.4	43.2	40.7		
			ln(%ee)	3.98	3.77	3.70	0.071	9.8
3	20mM	2	%ee	52.2	41.5	37.0		
			ln(%ee)	3.95	3.73	3.61	0.084	8.3
4	30mM	2	%ee	44.1	32.9	26.6		
			ln(%ee)	3.79	3.49	3.28	0.14	5.0
5	20mM	3	%ee	47.1	34.4	28.9		
			ln(%ee)	3.85	3.54	3.36	0.13	5.3
6	20mM	4	%ee	40.7	28.6	19.3		
			ln(%ee)	3.71	3.35	2.96	0.19	3.6

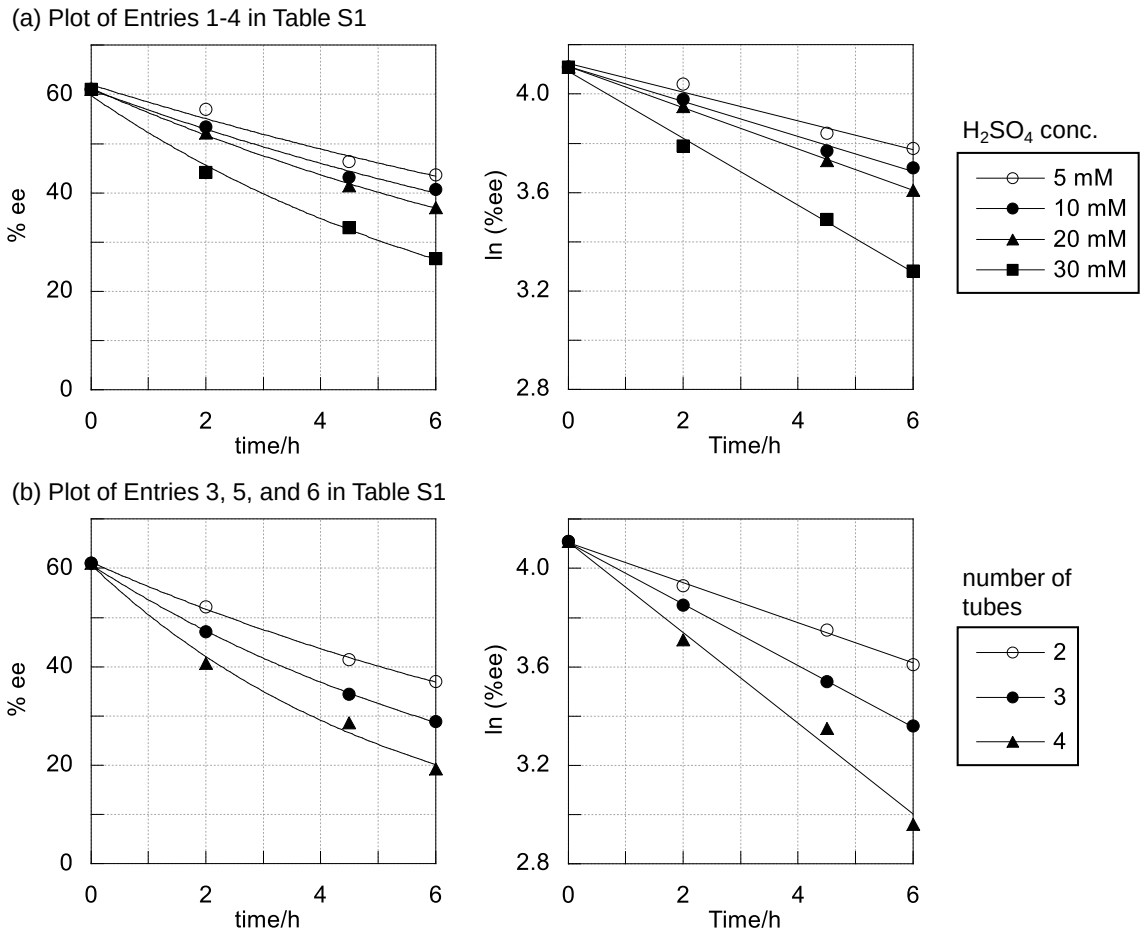


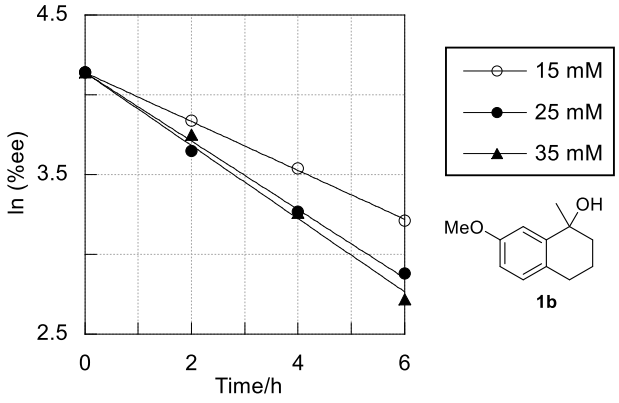
Figure S1. Time course of % ee and its ln-plot in racemization of **1a**.

Table S2. Time course of %ee in H_2SO_4-catalysed biphasic racemization of **1b**–**1f**

(a) Racemization of **1b**

H_2SO_4 conc.	15 mM	25 mM	35 mM
Time	ln(%ee)		
0 h	4.14	4.14	4.14
2.0 h	3.84	3.65	3.75
4.0 h	3.54	3.27	3.26
6.0 h	3.21	2.88	2.72
k_{rac} / h^{-1} [a]	0.15 (n.d.)	0.22 (6)	0.23 (10)

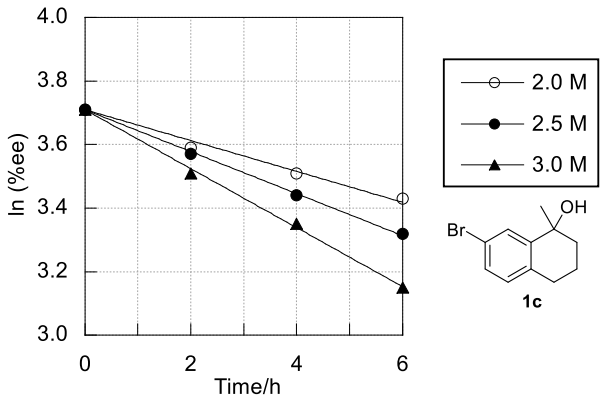
[a] Combined yield of **2b** and **2b'** at 24 h are shown in the parentheses. n.d.: not detected.



(b) Racemization of **1c**

H_2SO_4 conc.	2.0 M	2.5 M	3.0 M
Time	ln(%ee)		
0 h	3.71	3.71	3.71
2.0 h	3.59	3.57	3.51
4.0 h	3.51	3.44	3.35
6.0 h	3.43	3.32	3.15
k_{rac} / h^{-1} [a]	0.048 (n.d.)	0.066 (20)	0.093 (24)

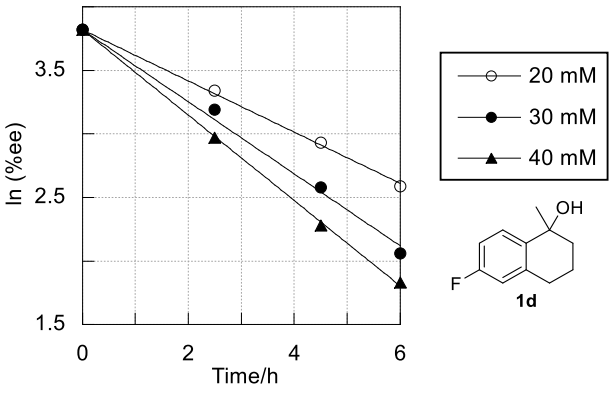
[a] Combined yield of **2b** and **2b'** at 24 h are shown in the parentheses. n.d.: not detected.



(c) Racemization of **1d**

H_2SO_4 conc.	20 mM	30 mM	40 mM
Time	ln(%ee)		
0 h	3.82	3.82	3.82
2.5 h	3.34	3.19	2.97
4.5 h	2.93	2.58	2.28
6.0 h	2.59	2.06	1.83
k_{rac} / h^{-1} [a]	0.20 (2)	0.28 (6)	0.33 (14)

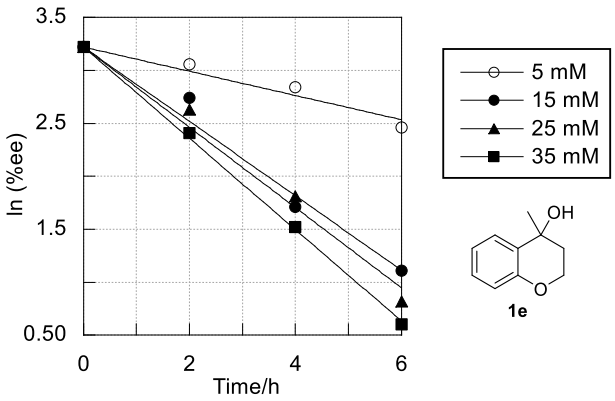
[a] Combined yield of **2b** and **2b'** at 24 h are shown in the parentheses. n.d.: not detected.



(d) Racemization of **1e**

H_2SO_4 conc.	5 mM	15 mM	25 mM	35 mM
Time	ln(%ee)			
0 h	3.22	3.22	3.22	3.22
2.0 h	3.06	2.74	2.63	2.41
4.0 h	2.84	1.71	1.81	1.52
6.0 h	2.46	1.11	0.82	0.60
k_{rac} / h^{-1} [a]	0.11 (n.d.)	0.35 (n.d.)	0.38 (2)	0.43 (7)

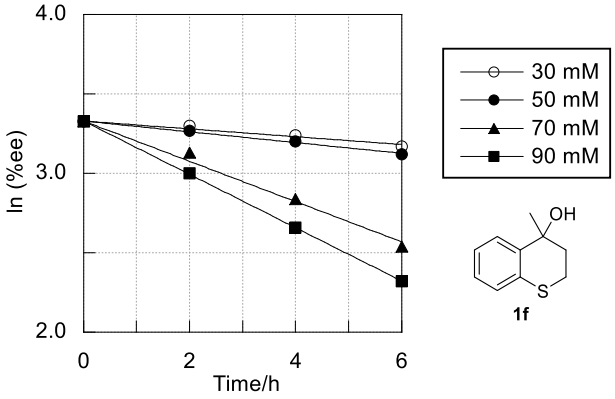
[a] Combined yield of **2b** and **2b'** at 24 h are shown in the parentheses. n.d.: not detected.



(e) Racemization of **1f**

H_2SO_4 conc.	30 mM	50 mM	70 mM	90 mM
Time	ln(%ee)			
0 h	3.33	3.33	3.33	3.33
2.0 h	3.30	3.27	3.13	3.00
4.0 h	3.24	3.20	2.84	2.66
6.0 h	3.17	3.12	2.54	2.32
k_{rac} / h^{-1} [a]	0.024 (n.d.)	0.0.35 (n.d.)	0.13 (5)	0.17 (9)

[a] Combined yield of **2b** and **2b'** at 24 h are shown in the parentheses. n.d.: not detected.



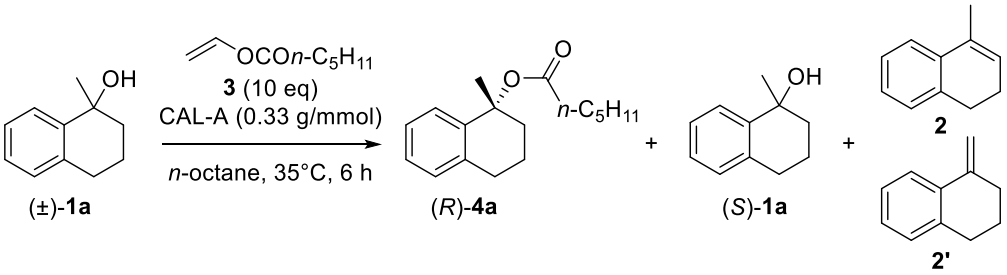
5. CAL-A-catalysed kinetic resolution of 1a in flow reactor

5.1. Investigation of filler

The kinetic resolution of (±)-**1a** with **3** was investigated under flow conditions. While the yield was 30% after 6 h when the lipase was packed alone in the column, the yield of **4a** reached 45% when Celite was mixed with the lipase as a filler to increase the residence time (Table S3).[6] In contrast, other fillers were found to be unsuitable. That is, using Florisil and mesoporous silica as the filler resulted in considerable amounts of side products **2a** and **2a'** with low yields of **4a**, probably because these fillers induced acid-mediated dehydration of **1a** and **4a**. The use of molecular sieves resulted in a low yield of **4a**, with a large amount of unreacted **1a** being recovered.

Experimental procedure: CAL-A beads (50 mg) were grinded in a mortar and mixed with the indicated filler. The mixture was then packed into an Omnifit® EZ SolventPlus™ column (6.6 mm × 100 mm) equipped with an adjustable end-piece, which was fastened to secure the packed material. The column

was fixed in a heating chamber (25°C) and connected to a 20-mL screw-capped vial (diameter: 27 mm) via 1/16" TPFE tubes. A solution of (±)-**1a** (0.15 mmol) and **3** (10 eq, 1.5 mmol) in *n*-octane (3 mL) was prepared and circulated through the column at a flow rate of 50 μL/min using a roller pump (Minato Concept, Inc., MCRP 204). After 6 h, the column was washed by flowing EtOAc (4 mL) and the combined organic solvent was concentrated under reduced pressure. The residue was analyzed by ^{1}H NMR using 1,4-dimethoxybenzene as an internal standard to determine the yield.



Entry	Filler	%Yield of **4a**
1[b]	None	30
2	Celite	45
3	Florisil	15 + **2**/**2'**
4	Mesoporous silica	4 + **2**/**2'**
5	MS4A	8 + **2**/**2'**

[a] Unless otherwise noted, the reaction was conducted using **1a** (0.15 mmol) and **3** (1.5 mmol) in *n*-octane (3.0 mL). The reactor was packed with CAL-A (50 mg) and the indicated filler (300 mg). [b] A ø2.2 mm PTFE tube was used as the column reactor.

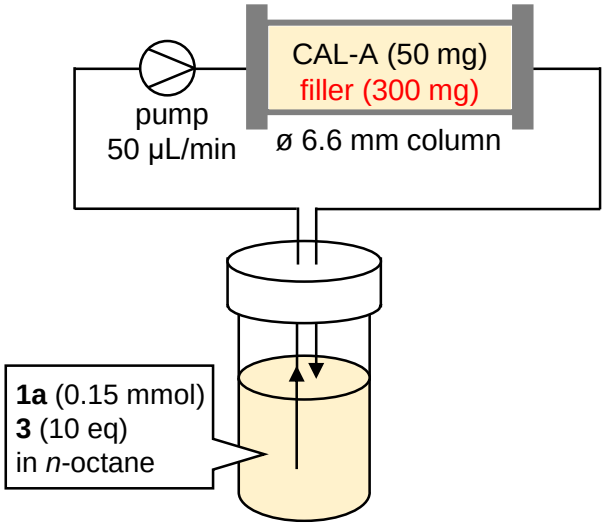


Figure S2. Effects of filler on the CAL-A-catalysed flow esterification reaction[a]

5.2 Investigation of additives in flow experiment

The effects of additives on the yield of **4a** in the CAL-A-catalysed kinetic resolution of (±)-**1a** under continuous flow conditions were investigated (Fig. S3). The addition of the inorganic base Na_2CO_3 significantly improved the yield, and CAL-A retained high catalytic activity over a 6-h period (● vs ○). In contrast, the use of bile salts such as sodium taurocholate (■) and sodium deoxycholate (▲) in place of Na_2CO_3 was ineffective, despite their known effectiveness as surfactants in lipase-catalysed reactions in aqueous media.[7] Given that the kinetic resolution in Fig. S3 occurs in the organic phase using immobilized CAL-A, the beneficial effect of Na_2CO_3 can be attributed to its basicity. Specifically, Na_2CO_3 may enhance catalytic activity by neutralizing hexanoic acid, a side product of the hydrolytic reaction of vinyl ester **3**, which could otherwise deactivate the acid-labile lipase.[4]

The total amount of (*R*)-**4a** produced during the first 6 h of operation was 0.20 mmol in the presence of Na_2CO_3 and 0.14 mmol in its absence, using 50 mg of CAL-A (1340 U/g). Accordingly, the enzyme unit requirement per mmol of (*R*)-**4a** produced was calculated to be 3.4×10^2 U/mmol with Na_2CO_3 and 4.9×10^2 U/mmol without Na_2CO_3.

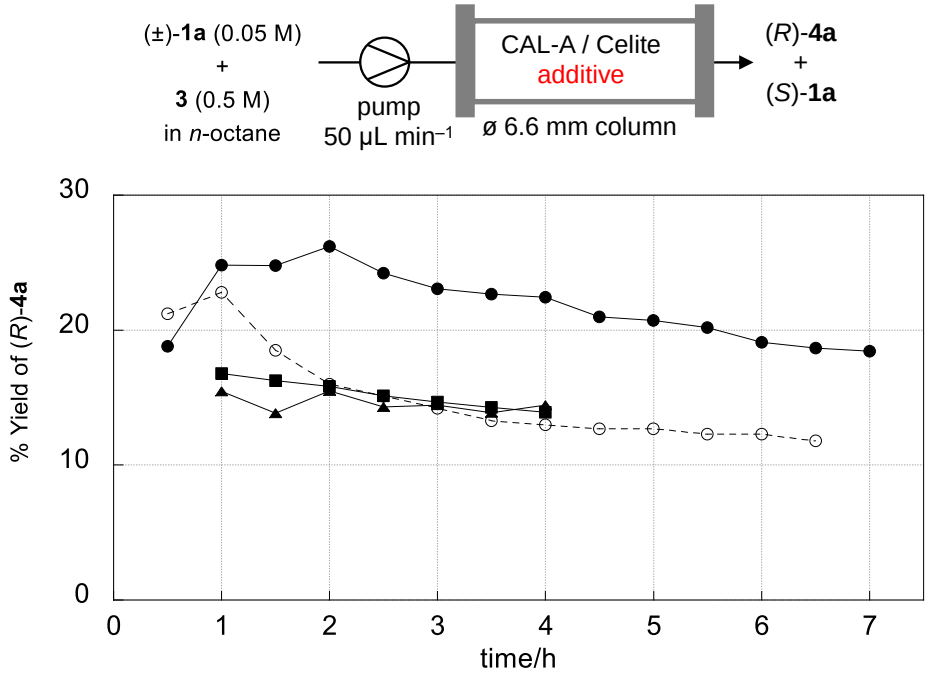


Figure S3. CAL-A-catalysed kinetic resolution of (±)-**1a** under flow conditions. The reaction was conducted using an *n*-octane solution containing (±)-**1a** (0.05 M) and **3** (0.5 M, 10 eq.) at a flow rate of 50 µL min^{-1} (residence time 20 min). The column reactor was packed with CAL-A (50 mg), Celite (330 mg), and the indicated additive (300 mg): (●) Na_2CO_3; (○) none; (■) sodium taurocholate; (▲) sodium deoxycholate.

Experimental procedure (Figures 2 and S3): CAL-A beads (50 mg) were grinded in a mortar and mixed with Celite (450 mg), and Na_2CO_3 or the indicated additive (300 mg). The mixture was packed into an Omnifit® EZ SolventPlus™ column (6.6 mm × 100 mm) equipped with an adjustable end-piece, which was fastened to secure the packed material. The column was fixed in a heating chamber (25°C), and connected to a fraction collector (ADVANTEC CHF122SC) and a 25-mL syringe on a syringe pump (YMC YSP-301) using 1/16" TPFE tubes. A solution of (±)-**1a** (0.05 M) and **3** (0.5 M) in *n*-octane was prepared and continuously pumped through the column reactor. The outlet solution was collected in fractions every 30 min using a fraction collector. Each collected fraction was subjected to chiral HPLC analysis. Since no side products and decomposition were observed in ^{1}H NMR analysis of each crude mixture, the yield of (*R*)-**4a** was calculated based on the ee values of **1a** and **4a** using the following equation:[8,9]

Yield (%) = ee(**1a**) / [ee(**1a**) + ee(**4a**)] × 100

Reusability of CAL-A

The reusability of CAL-A in the kinetic resolution was investigated under the recycle flow conditions (Figure S4). When a column reactor packed with fresh CAL-A was used, the yield of **4a** reached 40% at 8 h (●). In contrast, a significantly slower reaction rate was observed when the column reactor reused from the previous experiment was employed (○).

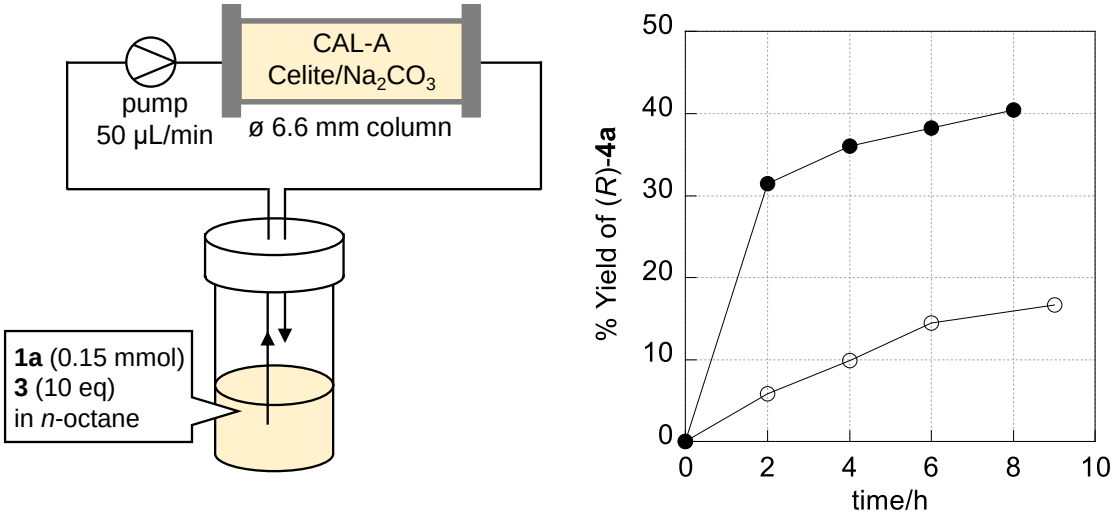


Figure S4. Reuse of CAL-A-packed column in kinetic resolution of **(±)-1a**. The reaction was conducted using an *n*-octane solution (3.3 mL) containing (±)-**1a** (0.15 mmol) and **3** (1.5 mmol) at a flow rate of 50 μL min^{-1} (residence time 20 min). The column reactor was packed with CAL-A (50 mg), Celite (330 mg), and Na_2CO_3 (200 mg): (●) freshly prepared column; (○) reused column.

6. Lipase/H_2SO_4-cocatalysed biphasic DKR of (±)-1

Experimental procedure using H_2SO_4 solution sealed in PDMS thimbles: An Omnifit® EZ SolventPlus™ column (6.6 mm × 100 mm) was charged with $MgSO_4$ (140 mg), and then a mixture of grinded CAL-A (50 mg), Celite (330 mg) and Na_2CO_3 (200 mg). The adjustable end-piece was fastened to secure the packed material. The column was connected to a 20-mL screw-capped vial (27-mm diameter) by 1/16" TPFE tubes. A solution of (±)-**1a** (0.15 mmol) and **3** (10 eq, 1.5 mmol) in *n*-octane (3.3 mL) was added to the vial, and PDMS thimble containing aq. H_2SO_4 (300 μL × 4) were immersed into the solution. The column and the vial were fixed in a heating chamber (25 °C), and the solution was circulated at a flow rate of 50μL/min using a roller pump with gentle stirring (Figure S3). After 26 h, the column was washed by flowing EtOAc (4 mL). H_2SO_4 solution in PDMS thimbles were collected and neutralized by aq. $NaHCO_3$. The organic solvent and the aqueous phase were combined and extracted with EtOAc (× 3). The combined organic layers were concentrated under reduced pressure. The residue was further concentrated using a Smart Evaporator C1 (BioChromato, Inc., Kanagawa,

Japan) to remove remaining vinyl hexanoate. The residue was purified by flash column chromatography using silica gel modified with aminopropyl groups (Wakogel® 50NH2, FUJIFILM Wako Pure Chemical, Tokyo, Japan) to give (*R*)-**4a** (91% isolated yield, >99% ee).

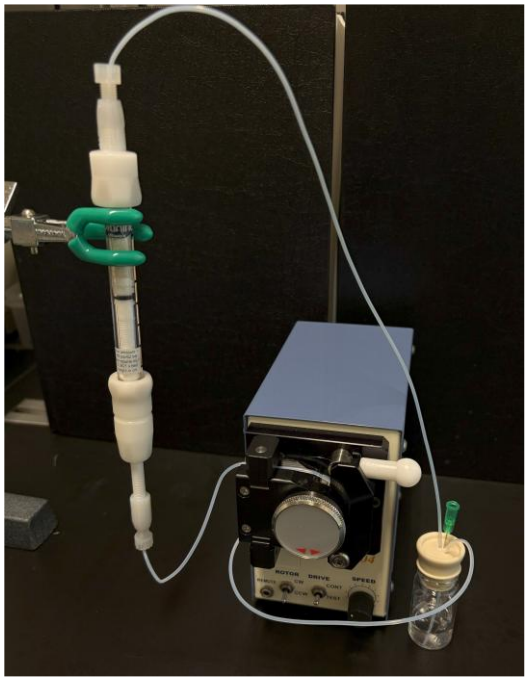
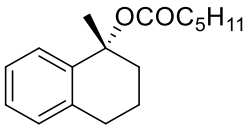


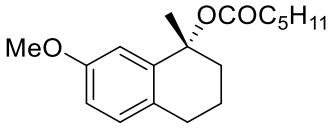
Figure S5. Setup for recycling flow reaction (heating chamber is not shown).

Experimental procedure of DKR in a Pickering emulsion: A water-in-oil Pickering emulsion was prepared according to a previously reported procedure.[10] Briefly, a mixture of silica nanoparticles (90 mg), *n*-octane (3.0 mL), and aqueous H_2SO_4 (7 mM, 0.90 mL) was homogenized in a 20 mm-diameter vial for 90 seconds at 20,000 rpm using a T10 basic ULTRA-TURRAX homogenizer (IKA) equipped with a S10N-5G dispersing tool (ø = 5 mm). After the emulsion droplets precipitated, the supernatant was removed, and a solution of (±)-**1a** (0.15 mmol) and **3** (10 equiv., 1.5 mmol) in *n*-octane (3.0 mL) was gently added to the vial. Anhydrous $MgSO_4$ (400 mg) was then placed on top of the emulsion layer. The reaction was initiated by adding CAL-A (50 mg) on top of the $MgSO_4$, and the vial was left standing in a heating chamber at 35 °C without stirring. After 26 h, solid $NaHCO_3$ was added to neutralize the acid. The mixture was diluted with EtOAc and filtered through a pad of $MgSO_4$. The combined organic layer was concentrated under reduced pressure, and the residue was analyzed by ^{1}H NMR using 1,4-dimethoxybenzene as an internal standard to determine the yield of (*R*)-**4a** (57% yield, >99% ee).

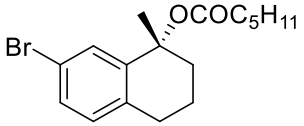


(*R*)-1-Methyl-1,2,3,4-tetrahydronaphthalen-1-yl hexanoate (4a)[4]: Purified by column chromatography using Wakogel 50NH2 (hexane/EtOAc = 10:1); 91% yield; a colorless oil; $[\alpha]^{27}{}_D = -28$

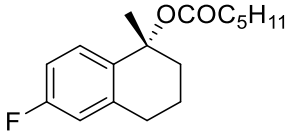
(*c* 1.00, CH_3OH) (lit.[4] $[\alpha]^{23}_D = -25$ (*c* 0.95, CH_3OH), 99% ee, *R*); HPLC analysis CHIRALPAK IJ-3 (hexane/*i*-PrOH = 98:2 1 mL/min, 220 nm, 25°C) 4.6 (*S*), 5.5 (*R*) min (>99% ee); ^{1}H NMR (500 MHz, $CDCl_3$) δ 7.36 (dd, *J* = 7.3, 1.9 Hz, 1H), 7.19-7.13 (m, 2H), 7.08-7.06 (m, 1H), 2.91-2.85 (m, 1H), 2.74 (dt, *J* = 16.5, 4.8 Hz, 1H), 2.54 (td, *J* = 12.4, 3.2 Hz, 1H), 2.29-2.19 (m, 2H), 2.14-2.09 (m, 1H), 1.99-1.93 (m, 1H), 1.82-1.75 (m, 1H), 1.73 (s, 3H), 1.60-1.53 (m, 2H), 1.34-1.23 (m, 4H), 0.88 (t, *J* = 7.0 Hz, 3H); ^{13}C NMR (126 MHz, $CDCl_3$) δ 172.8, 140.4, 136.5, 128.7, 127.0, 126.0, 125.8, 81.1, 35.5, 34.5, 31.2, 29.5 (2C), 24.7, 22.3, 20.9, 13.9.



(*R*)-7-Methoxy-1-methyl-1,2,3,4-tetrahydronaphthalen-1-yl hexanoate (4b)[4]: Purified by column chromatography using Wakogel 50NH2 (hexane/EtOAc = 10:1); 87% yield; a colorless oil; $[\alpha]^{28}_D = -64$ (*c* 1.03, CH_3OH) (lit.[4] $[\alpha]^{23}_D = -53$ (*c* 0.72, CH_3OH), 99% ee, *R*); HPLC analysis CHIRALPAK IC-3 (hexane/*i*-PrOH = 98:2, 1 mL/min, 220 nm, 25°C) 6.3 (*S*), 7.5 (*R*) min (>99% ee); ^{1}H NMR (500 MHz, $CDCl_3$) δ 6.99 (d, J = 8.3 Hz, 1H), 6.88 (d, J = 2.7 Hz, 1H), 6.73 (dd, J = 8.4, 2.7 Hz, 1H), 3.78 (s, 3H), 2.83-2.77 (m, 1H), 2.70-2.65 (m, 1H), 2.54-2.49 (m, 1H), 2.30-2.20 (m, 2H), 2.12-2.07 (m, 1H), 1.97-1.91 (m, 1H), 1.79-1.73 (m, 1H), 1.72 (s, 3H), 1.61-1.55 (m, 2H), 1.35-1.24 (m, 4H), 0.88 (t, J = 6.9 Hz, 2H); ^{13}C NMR (126 MHz, $CDCl_3$) δ 172.7, 157.8, 141.5, 129.6, 128.7, 112.9, 111.0, 81.2, 55.2, 35.5, 34.3, 31.3, 29.7, 28.7, 24.7, 22.3, 21.1, 13.9.

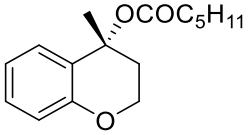


(*R*)-7-Bromo-1-methyl-1,2,3,4-tetrahydronaphthalen-1-yl hexanoate (4c)[4]: Purified by column chromatography using Wakogel 50NH2 (hexane/EtOAc = 10:1); 56% yield; a colorless oil; $[\alpha]^{29}_D = -68$ (*c* 1.03, CH_3OH) (lit.[4] $[\alpha]^{23}_D = -59$ (*c* 0.68, CH_3OH), 99% ee, *R*); HPLC analysis CHIRALPAK IJ-3 (hexane/*i*-PrOH = 99:1, 0.5 mL/min, 220 nm, 25°C) 9.5 (*S*), 10.7 (*R*) min (>99% ee); ^{1}H NMR (500 MHz, $CDCl_3$) δ 7.44 (d, *J* = 2.0 Hz, 1H), 7.25 (dd, *J* = 8.3, 2.0 Hz, 1H), 6.94 (d, *J* = 8.3 Hz, 1H), 2.84-2.77 (m, 1H), 2.68 (dt, *J* = 16.6, 4.5 Hz, 1H), 2.51 (td, *J* =12.5, 3.4 Hz, 1H), 2.26 (t, J = 7.4 Hz, 2H), 2.09-2.05 (m, 1H), 1.99-1.92 (m, 1H), 1.82-1.70 (m, 1H), 1.68 (s, 3H), 1.62-1.54 (m, 2H), 1.36-1.23 (m, 4H), 0.89 (t, *J* = 7.0 Hz, 3H); ^{13}C NMR (126 MHz, $CDCl_3$) δ 172.7, 142.7, 135.4, 130.4, 130.0, 128.6, 119.6, 80.4, 35.4, 34.0, 31.2, 29.8, 29.0, 24.7, 22.4, 20.8, 13.9.

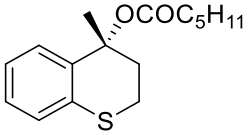


(*R*)-6-Fluoro-1-methyl-1,2,3,4-tetrahydronaphthalen-1-yl hexanoate (4d)[4]: Purified by column chromatography using Wakogel 50NH2 (hexane/EtOAc = 10:1); 79% yield; a colorless oil; $[\alpha]^{29}_D = -31$

(*c* 0.99, CH_3OH) (lit.[4] $[\alpha]^{23}_D$ = −21 (*c* 0.82, CH_3OH), 97% ee, *R*); HPLC analysis CHIRALPAK IJ-3 (two columns connected in series, hexane/*i*-PrOH = 99:1, 0.3 mL/min, 220 nm, 15°C) 38.0 (*S*), 41.2 (*R*) min (>99% ee); ^{1}H NMR (500 MHz, $CDCl_3$) δ 7.33 (dd, *J* = 8.5, 5.9 Hz, 1H), 6.86 (td, *J* = 8.5, 2.5 Hz, 1H), 6.76 (dd, *J* = 9.5, 1.6 Hz, 1H), 2.90-2.83 (m, 1H), 2.71 (dt, *J* = 16.7, 4.9 Hz, 1H), 2.53 (td, *J* = 12.3, 3.1 Hz, 1H), 2.28-2.17 (m, 2H), 2.09-2.03 (m, 1H), 1.99-1.92 (m, 1H), 1.81-1.73 (m, 1H), 1.71 (s, 3H), 1.59-1.52 (m, 2H), 1.34-1.23 (m, 4H), 0.88 (t, *J* = 6.7 Hz, 3H); ^{13}C NMR (126 MHz, $CDCl_3$) δ 172.7, 161.5 (d, J_{C-F} = 245.6 Hz), 139.0 (d, J_{C-F} = 7.5 Hz), 136.2 (d, J_{C-F} = 3 Hz), 127.7 (d, J_{C-F} = 8.4 Hz), 114.7 (d, J_{C-F} = 20.4 Hz), 113.2 (d, J_{C-F} = 21.3 Hz), 80.6, 35.5, 34.4, 31.2, 29.7, 29.5, 24.6, 22.3, 20.7, 13.9; ^{19}F NMR (471 MHz, $CDCl_3$) δ −115.9 (td, *J* = 8.9, 5.9 Hz, 1F).



(*R*)-4-Methylchroman-4-yl hexanoate (4e)[4]: Purified by column chromatography using Wakogel 50NH2 (hexane/EtOAc = 10:1); 70% yield; a colorless oil; $[\alpha]^{29}_D$ = +10 (*c* 1.05, CH_3OH) (lit.[4] $[\alpha]^{24}_D$ = +10 (*c* 0.62, CH_3OH), 96% ee, *R*); HPLC analysis CHIRALPAK IC-3 (hexane/*i*-PrOH = 98:2, 1 mL/min, 220 nm, 25°C) 5.3 (*R*), 7.5 (*S*) min (95% ee); ^{1}H NMR (500 MHz, $CDCl_3$) δ 7.49 (dd, J = 7.8, 1.6 Hz, 1H), 7.20-7.17 (m, 1H), 6.94-6.91 (m, 1H), 6.82 (dd, J = 8.2, 1.2 Hz, 1H), 4.33-4.29 (m, 1H), 4.20-4.16 (m, 1H), 2.68-2.61 (m, 1H), 2.34-2.19 (m, 3H), 1.89 (s, 3H), 1.61-1.54 (m, 2H), 1.34-1.22 (m, 4H), 0.87 (t, J = 7.1 Hz, 3H); ^{13}C NMR (126 MHz, $CDCl_3$) δ 173.0, 153.8, 129.4, 127.7, 125.4, 120.3, 117.0, 76.2, 63.0, 35.5, 34.3, 31.2, 26.5, 24.7, 22.3, 13.9.



(*R*)-4-Methylthiochroman-4-yl hexanoate (4f)[4]: Purified by column chromatography using Wakogel 50NH2 (hexane/EtOAc = 10:1); 70% yield; a colorless oil; $[\alpha]^{29}_D$ = −8.4 (*c* 1.03, CH_3OH) (lit.[4] $[\alpha]^{24}_D$ = −8.4 (*c* 0.69, CH_3OH), 98% ee, *R*); HPLC analysis CHIRALPAK IC-3 (hexane/*i*-PrOH = 98:2, 1 mL/min, 220 nm, 25°C) 6.4 (*R*), 8.4 (*S*) min (97% ee); ^{1}H NMR (500 MHz, $CDCl_3$) δ 7.45 (d, *J* = 7.9 Hz, 1H), 7.11-7.09 (m, 2H), 7.08-7.03 (m, 1H), 3.11-3.03 (m, 2H), 2.85-2.76 (m, 1H), 2.39-2.35 (m, 1H), 2.32-2.23 (m, 2H), 1.79 (s, 3H), 1.62-1.55 (m, 2H), 1.35-1.24 (m, 4H), 0.88 (t, *J* = 7.0 Hz, 3H); ^{13}C NMR (126 MHz, $CDCl_3$) δ 172.6, 136.7, 132.3, 127.6, 126.60, 126.55, 124.1, 78.8, 35.4, 33.7, 31.2, 28.0, 24.7, 23.3, 22.3, 13.9.

7. References

1 A. L. Miller and N. B. Bowden, *J. Org. Chem.*, 2009, **74**, 4834–4840.

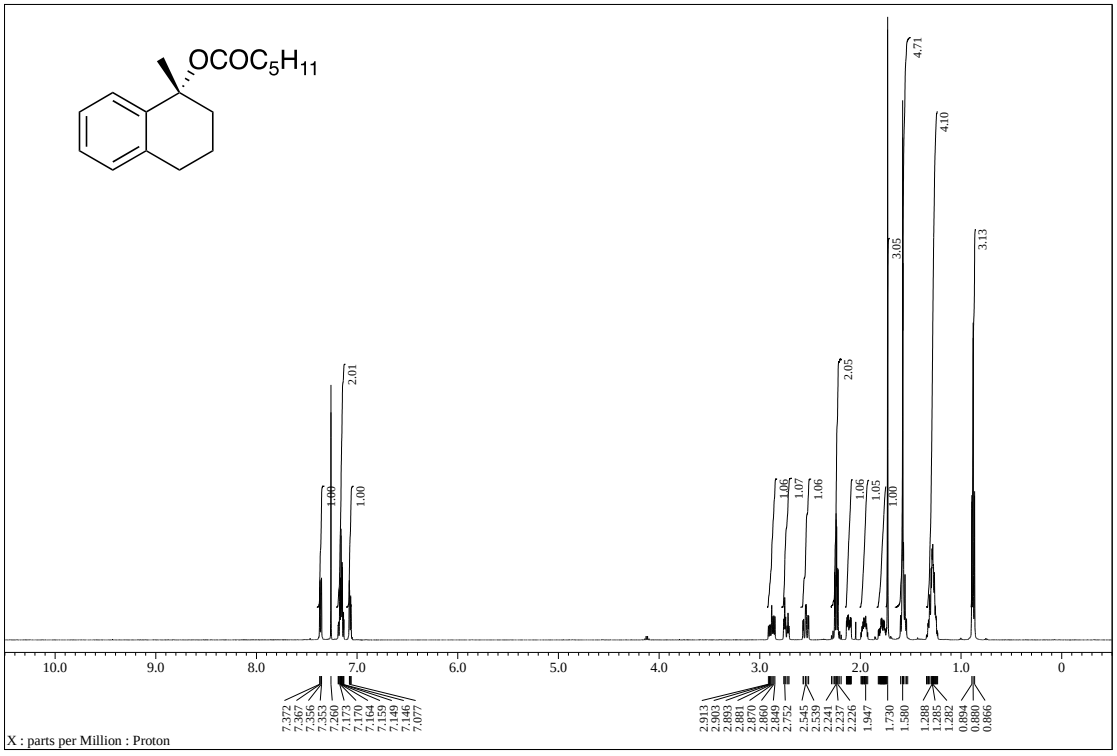
2 H. Sato, W. Hummel and H. Gröger, *Angew. Chem. Int. Ed.*, 2015, **54**, 4488–4492.

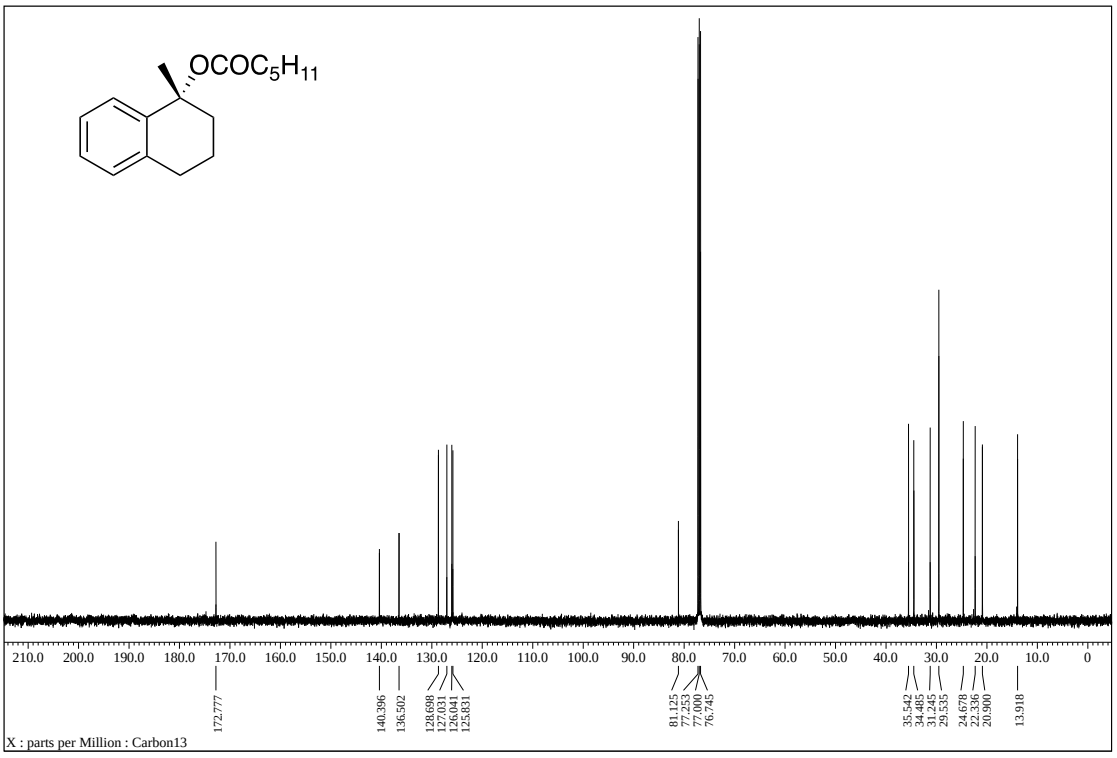
3 F. Kühn, S. Katsuragi, Y. Oki, C. Scholz, S. Akai and H. Gröger, *Chem. Commun.*, 2020, **56**,

2885–2888.
4 S. Horino, K. Wagner, A. Hummel, K. Kanomata, H. Gröger and S. Akai, *Eur. J. Org. Chem.*, 2024, **27**, e202400242.
5 C. Wolf, *Dynamic Stereochemistry of Chiral Compounds*, The Royal Society of Chemistry, Cambridge, 2008.
6 R. Ikeda, T. Nishio, K. Kanomata and S. Akai, *Chem. Pharm. Bull.*, 2024, **72**, 213–219.
7 H. Brockerhoff, *J. Biol. Chem.*, 1971, **246**, 5828–5831.
8 C. S. Chen, Y. Fujimoto, G. Girdaukas and C. J. Sih, *J. Am. Chem. Soc.*, 1982, **104**, 7294–7299.
9 J. M. Keith, J. F. Larrow and E. N. Jacobsen, *Adv. Synth. Catal.*, 2001, **343**, 5–26.
10 J. Moon, T. Kin, K. Mizuno, S. Akai and K. Kanomata, *ChemCatChem*, 2023, **15**, e202300878.

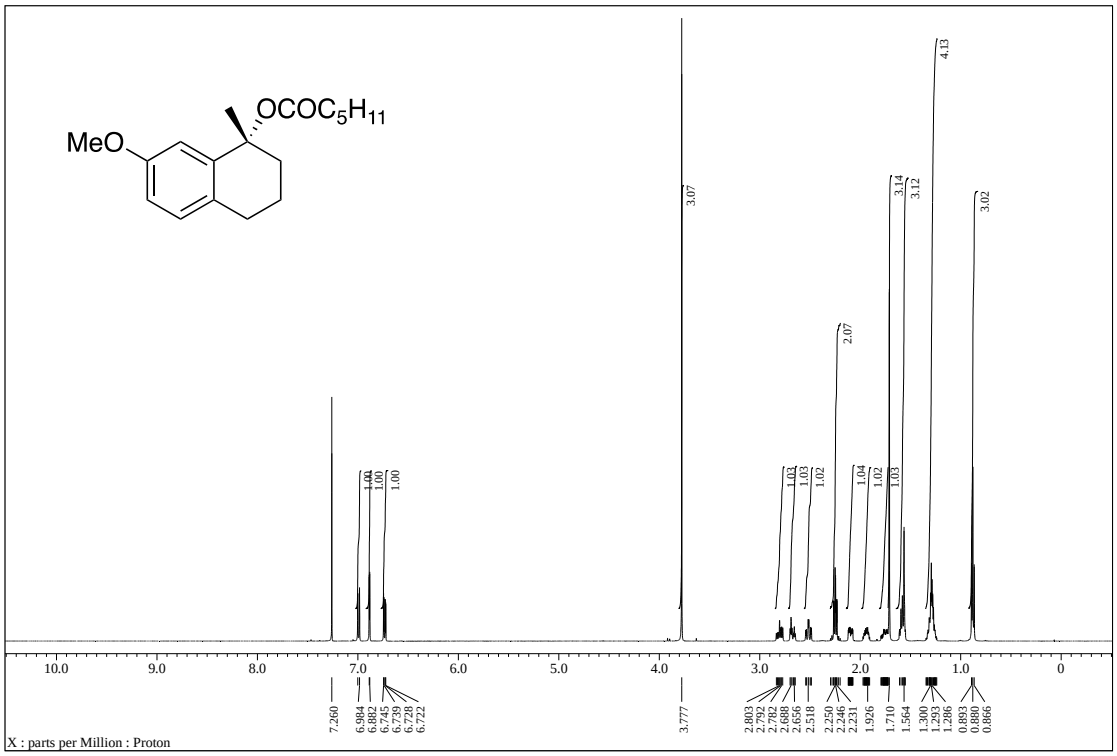
8. NMR and chiral HPLC chart

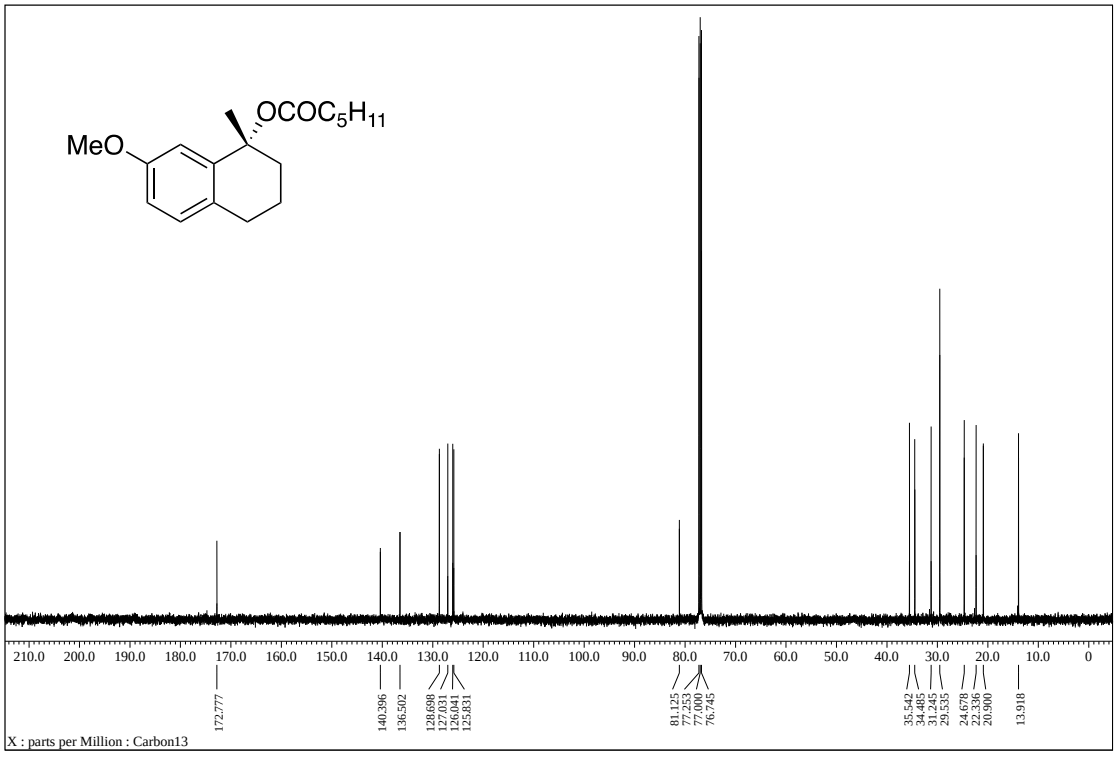
(*R*)-1-Methyl-1,2,3,4-tetrahydronaphthalen-1-yl hexanoate (4a)



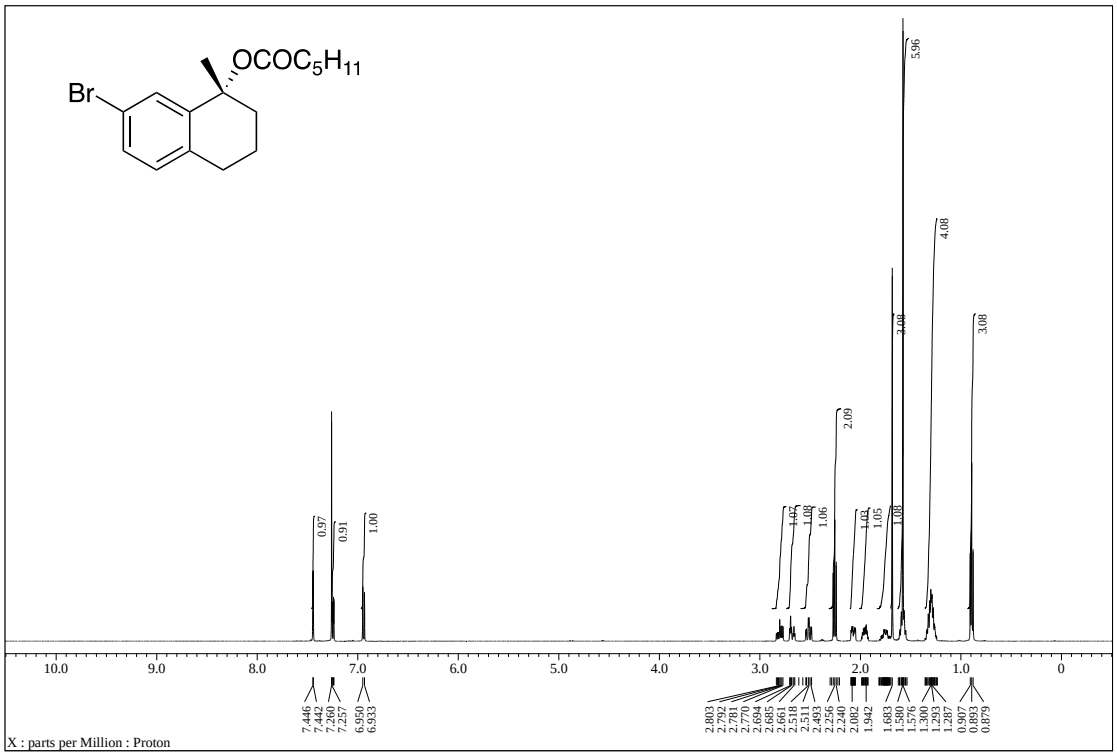


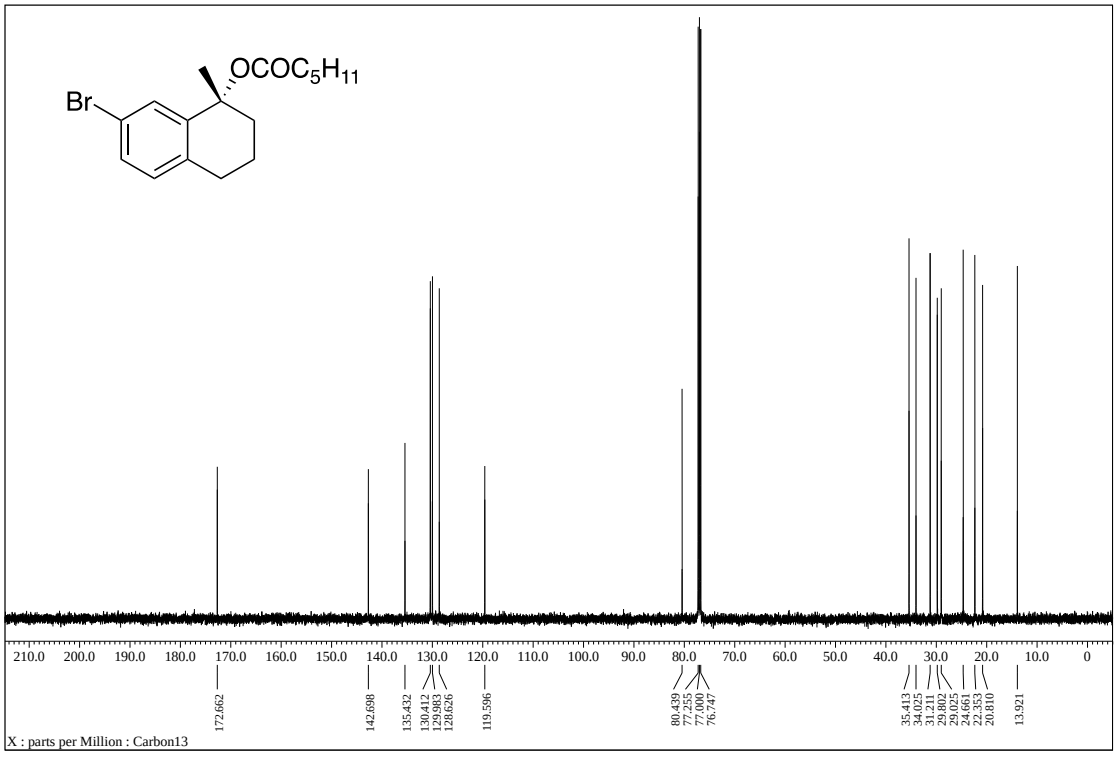
(*R*)-7-Methoxy-1-methyl-1,2,3,4-tetrahydronaphthalen-1-yl hexanoate (4b)



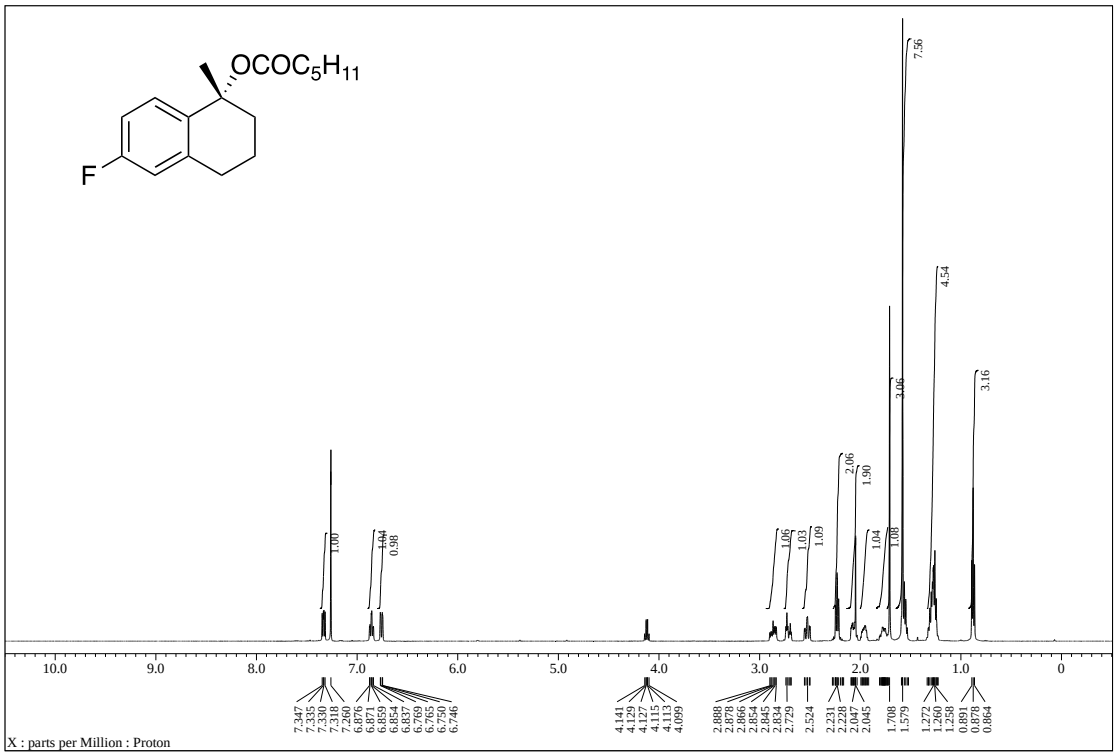


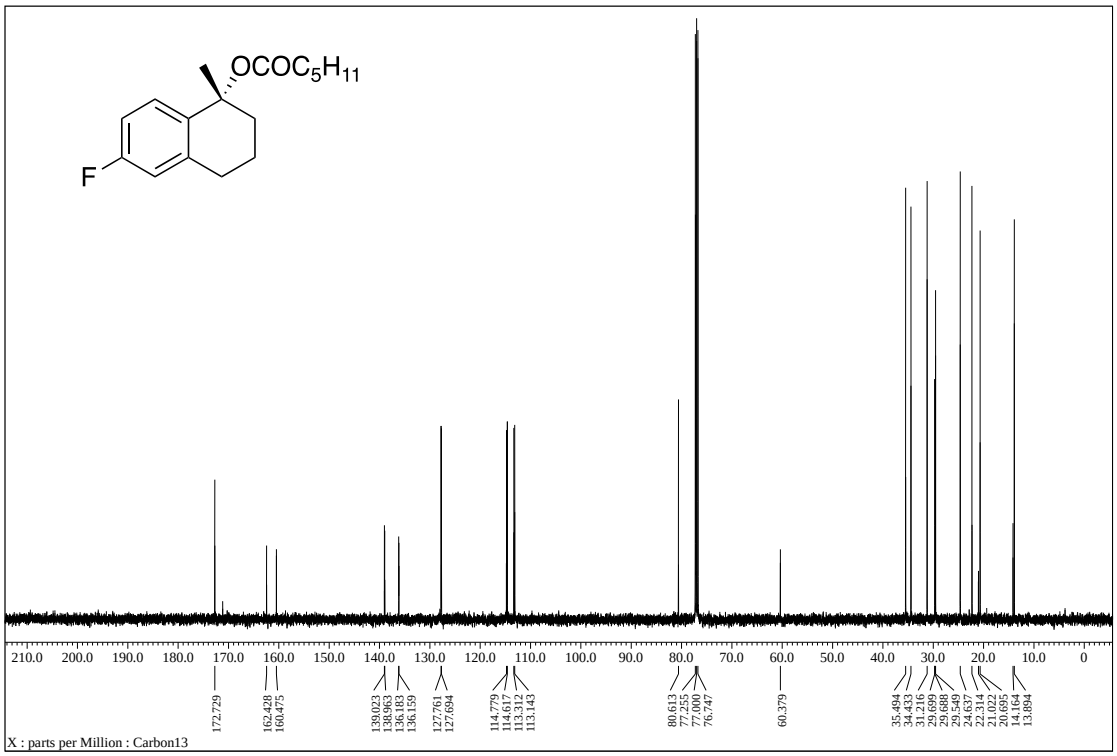
(*R*)-7-Bromo-1-methyl-1,2,3,4-tetrahydronaphthalen-1-yl hexanoate (4c)

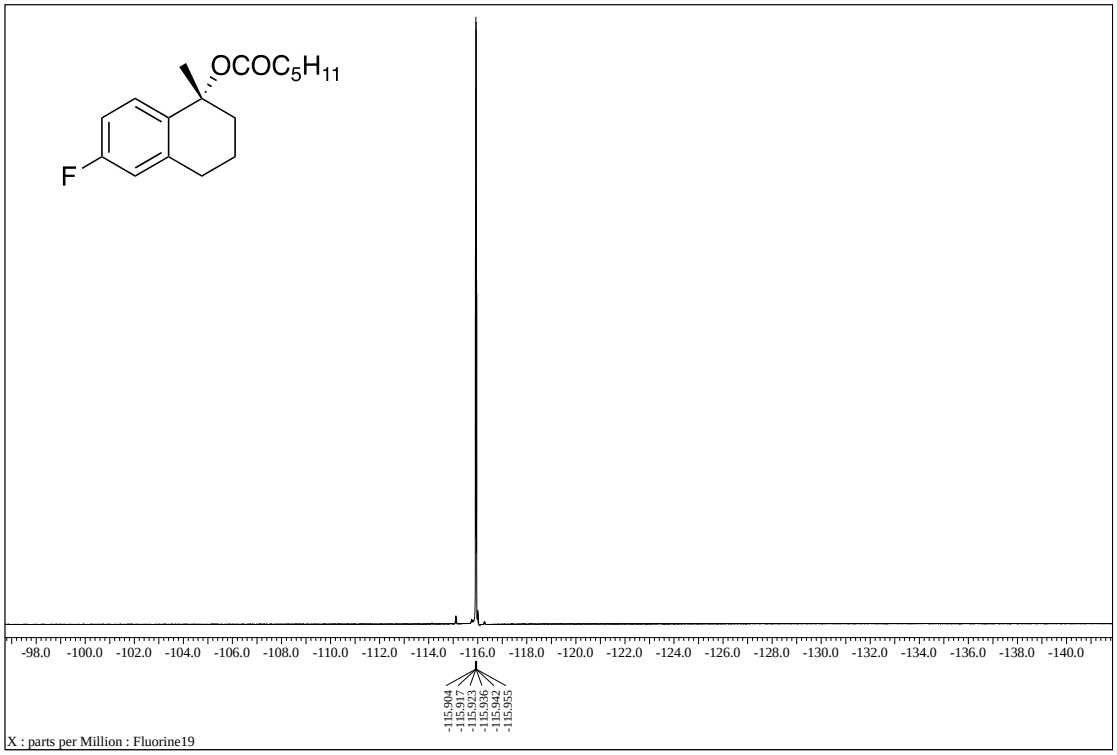




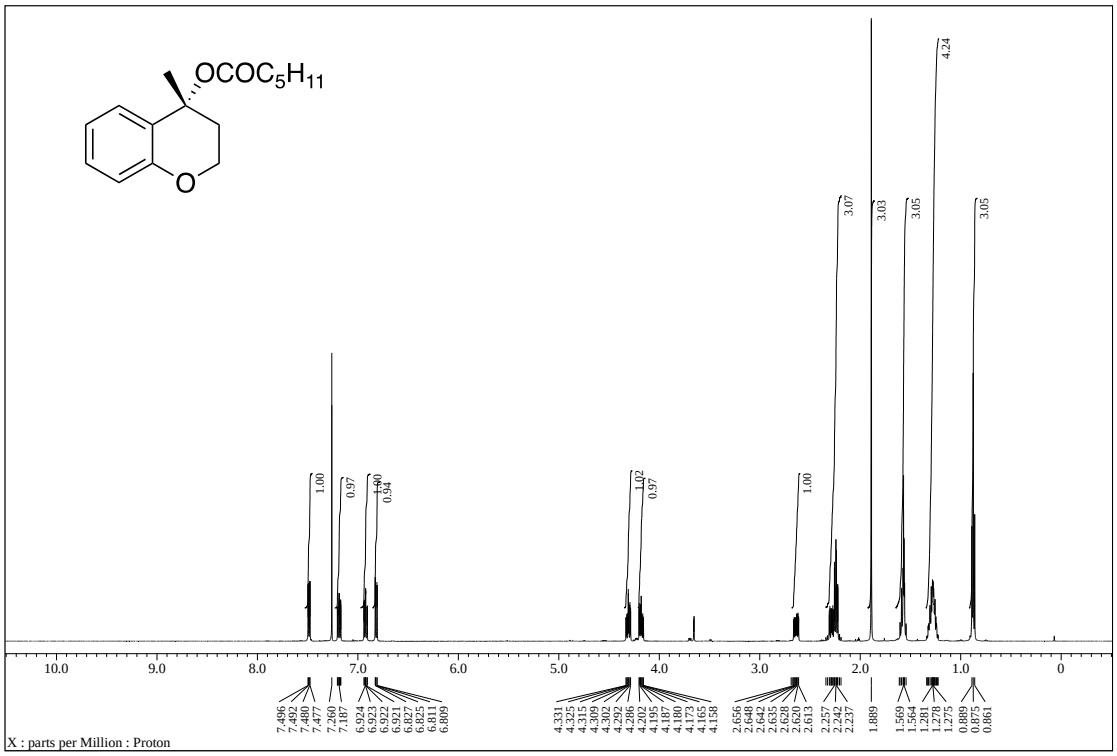
(*R*)-6-Fluoro-1-methyl-1,2,3,4-tetrahydronaphthalen-1-yl hexanoate (4d)

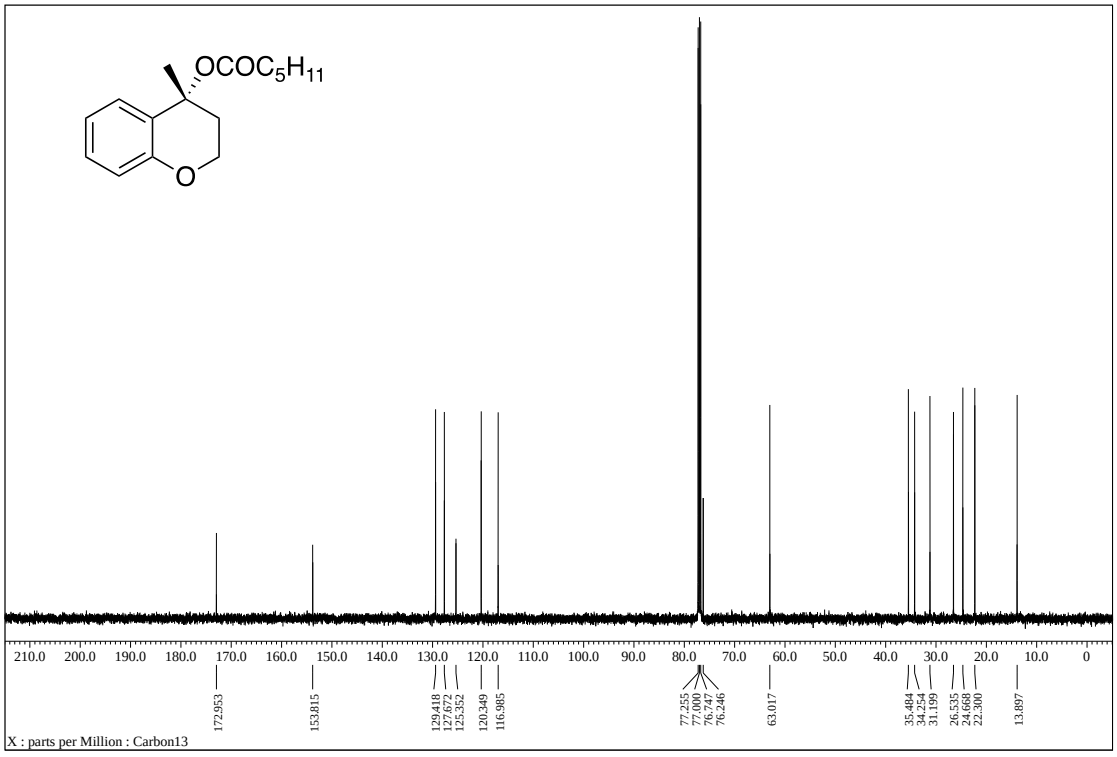




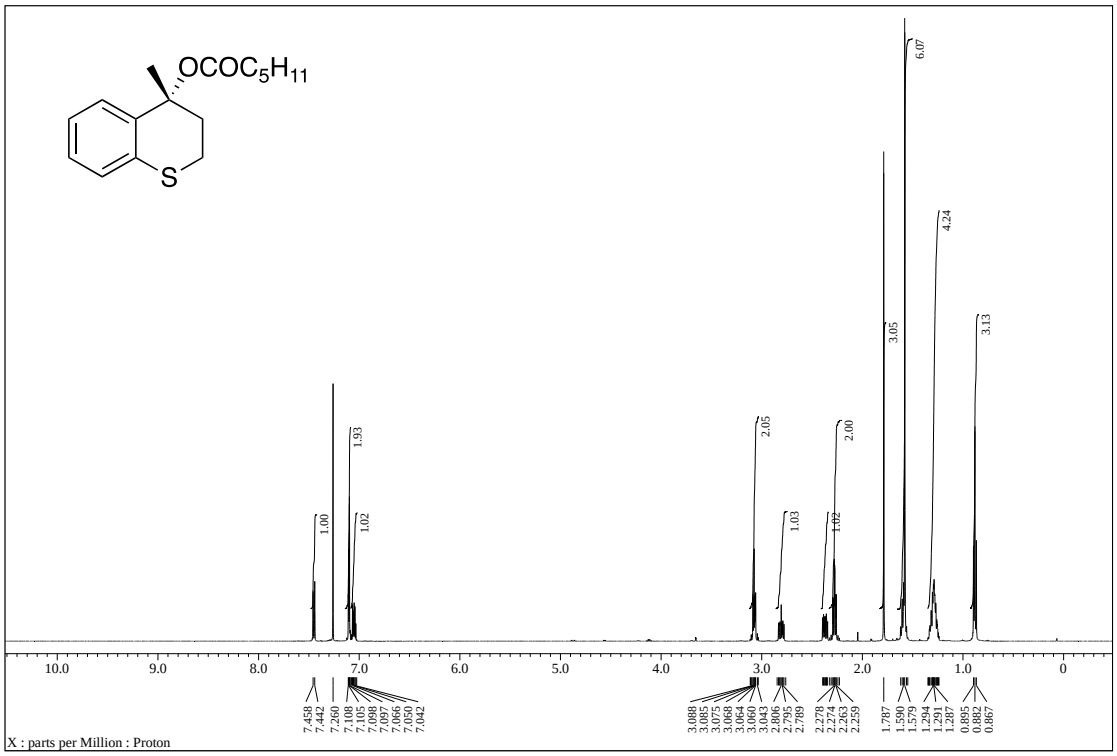

OCOC5H11
F
-98.0 -100.0 -102.0 -104.0 -106.0 -108.0 -110.0 -112.0 -114.0 -116.0 -118.0 -120.0 -122.0 -124.0 -126.0 -128.0 -130.0 -132.0 -134.0 -136.0 -138.0 -140.0
-115.904
-115.917
-115.923
-115.936
-115.942
-115.955
X : parts per Million : Fluorine19

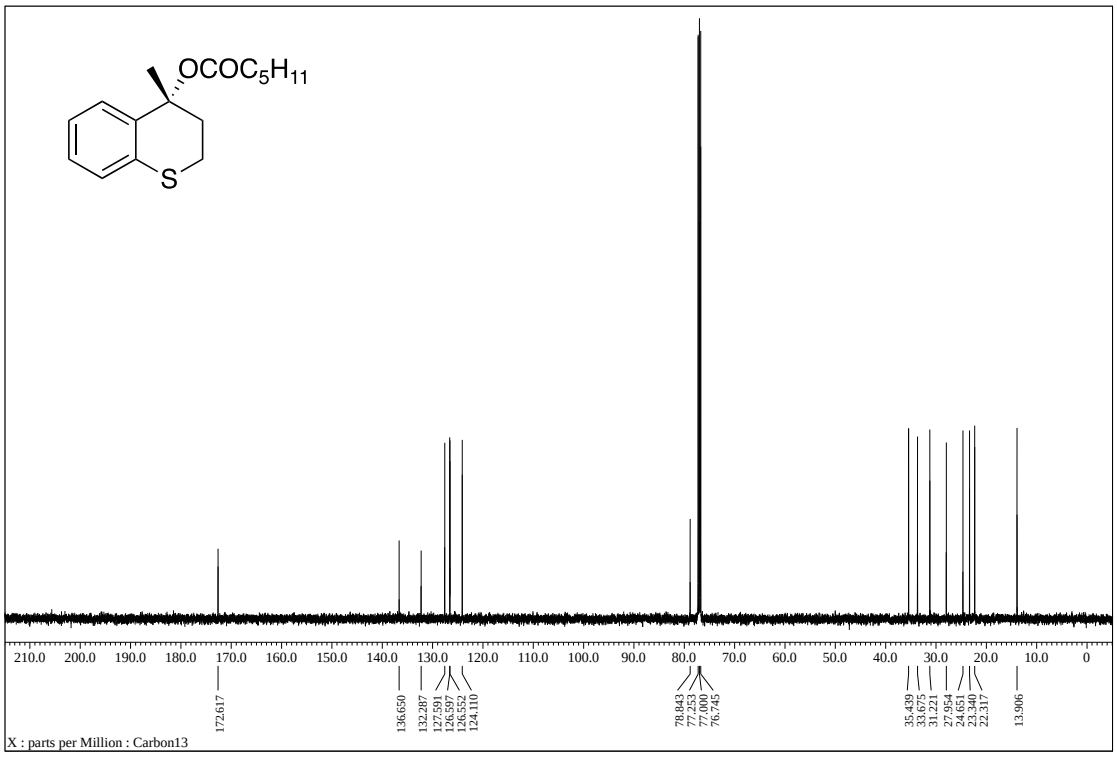
(*R*)-4-Methylchroman-4-yl hexanoate (4e)





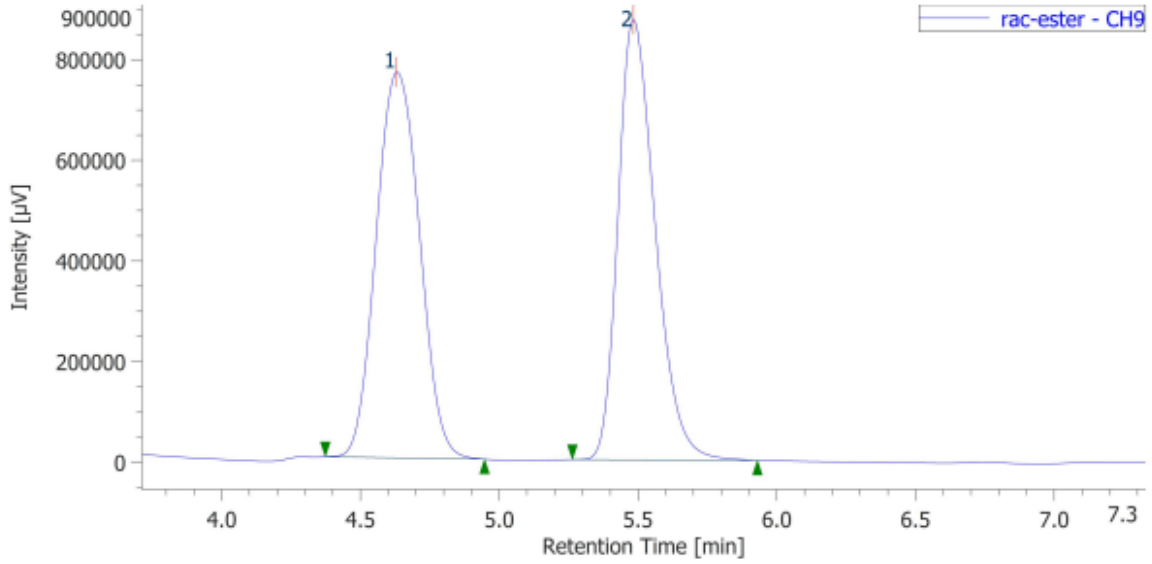
(*R*)-4-Methylthiochroman-4-yl hexanoate (4f)

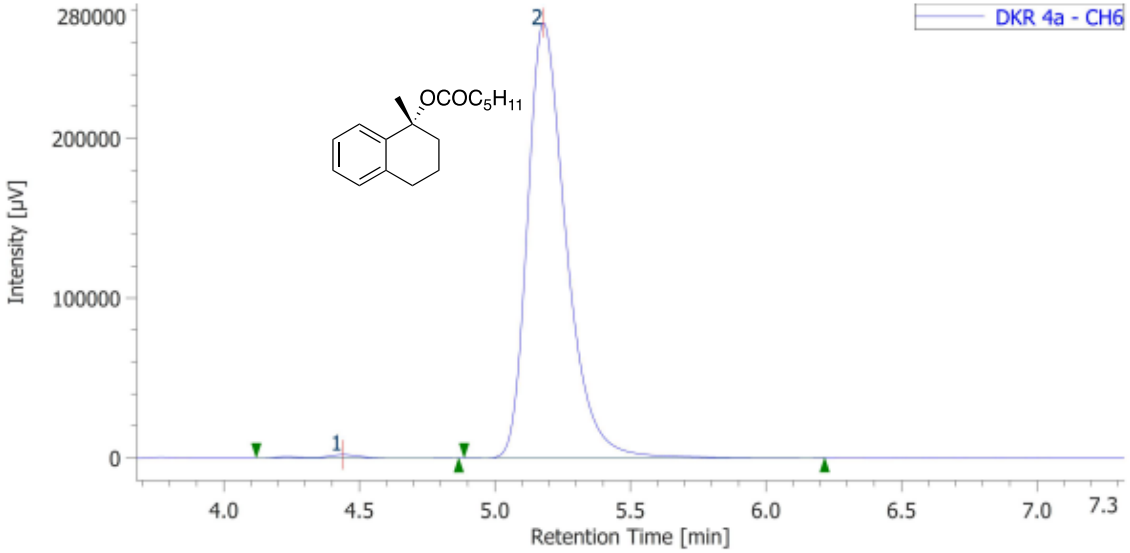




Chiral HPLC chart

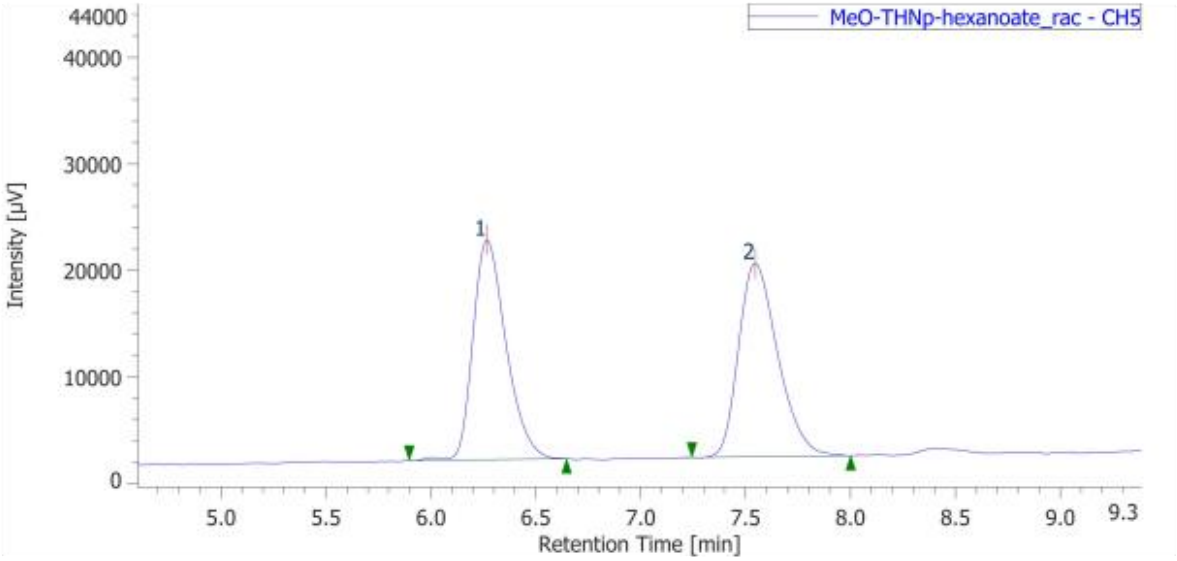
1-Methyl-1,2,3,4-tetrahydronaphthalen-1-yl hexanoate (4a)

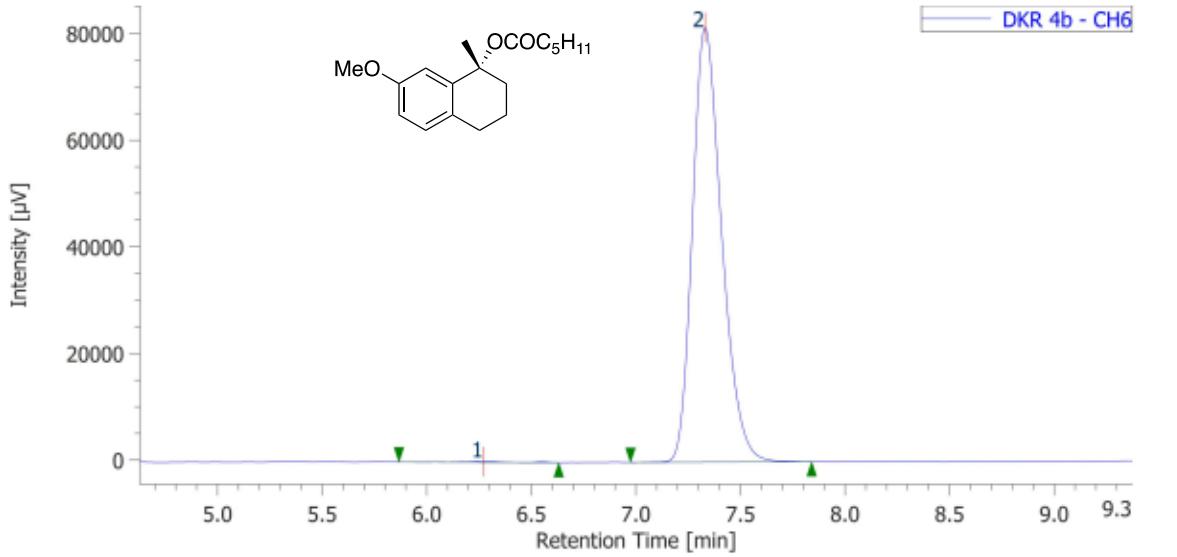




#	Peak Name	CH	tR [min]	Area [μV·sec]	Height [μV]	Area%	Height%	Quantity	NTP	Resolution	Symmetry Factor	Warning
1	Unknown	6	4.440	19043	1973	0.702	0.719	N/A	9122	3.397	0.762	
2	Unknown	6	5.180	2694518	272233	99.298	99.281	N/A	6821	N/A	1.368	

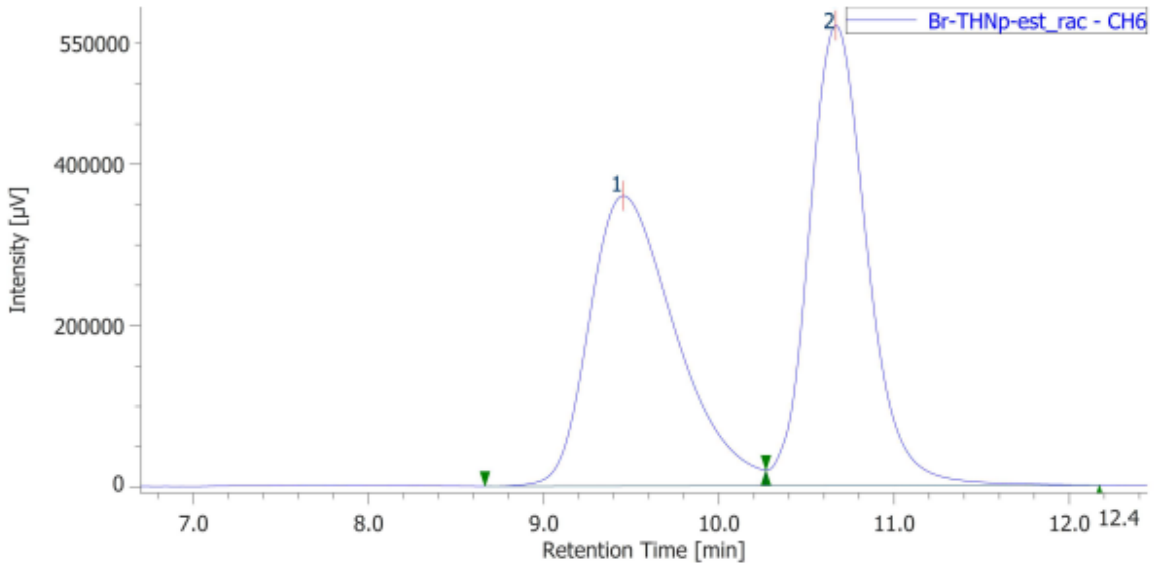
7-Methoxy-1-methyl-1,2,3,4-tetrahydronaphthalen-1-yl hexanoate (4b)

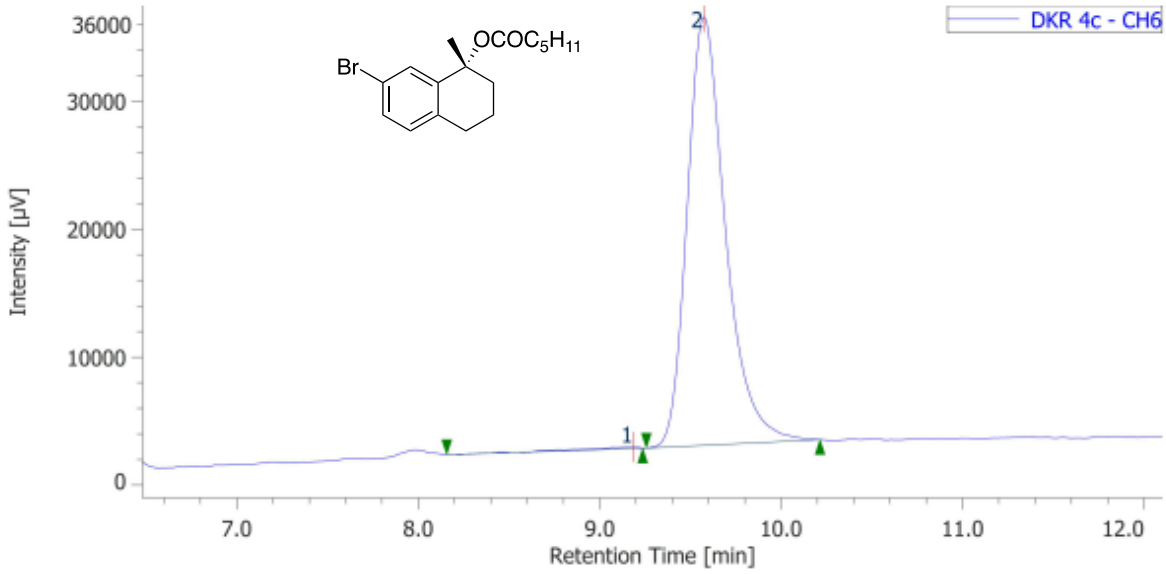




#	Peak Name	CH	tR [min]	Area [μV·sec]	Height [μV]	Area%	Height%	Quantity	NTP	Resolution	Symmetry Factor	Warning
1	Unknown	6	6.273	1679	146	0.211	0.179	N/A	1714	2.467	1.232	
2	Unknown	6	7.330	792758	81508	99.789	99.821	N/A	13473	N/A	1.282	

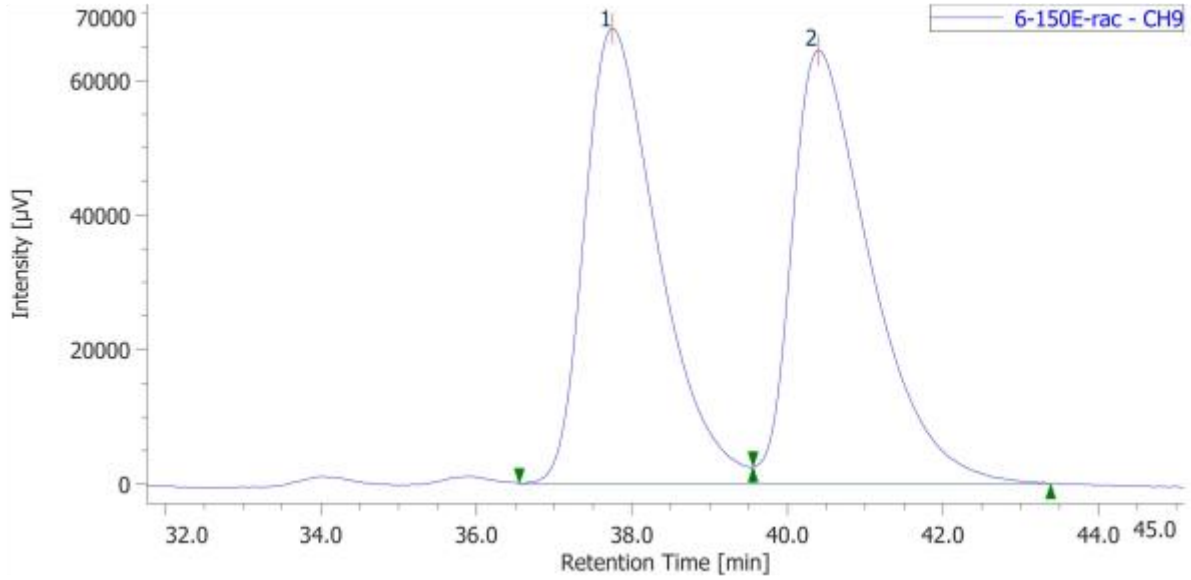
7-Bromo-1-methyl-1,2,3,4-tetrahydronaphthalen-1-yl hexanoate (4c)

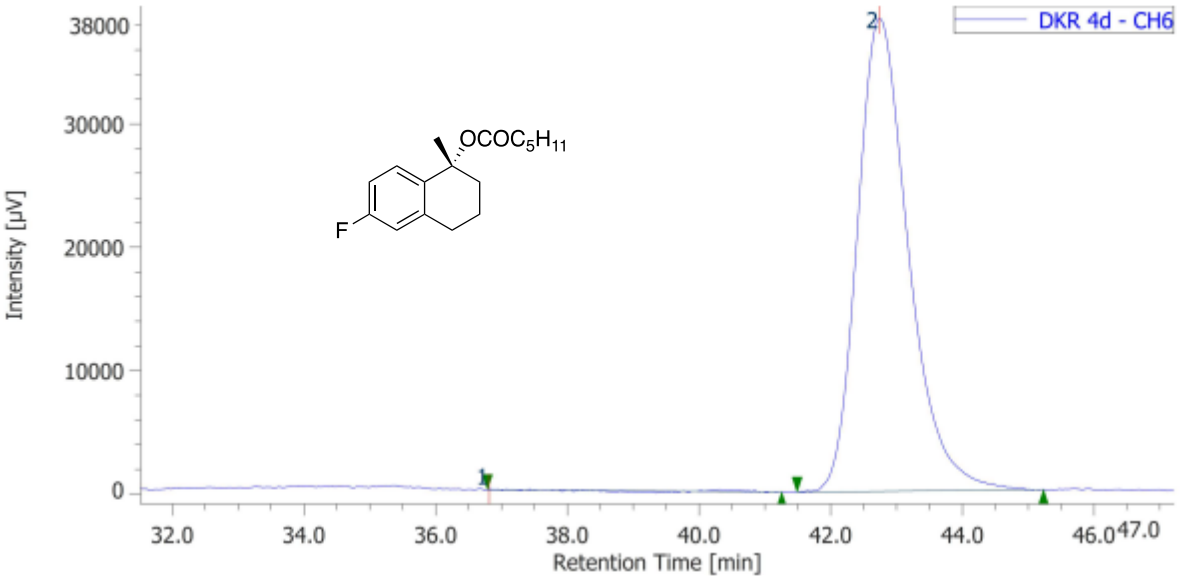




#	Peak Name	CH	tR [min]	Area [µV·sec]	Height [µV]	Area%	Height%	Quantity	NTP	Resolution	Symmetry Factor	Warning
1	Unknown	6	9.187	2807	102	0.568	0.303	N/A	771	0.458	0.526	
2	Unknown	6	9.573	491499	33454	99.432	99.697	N/A	10618	N/A	1.336	

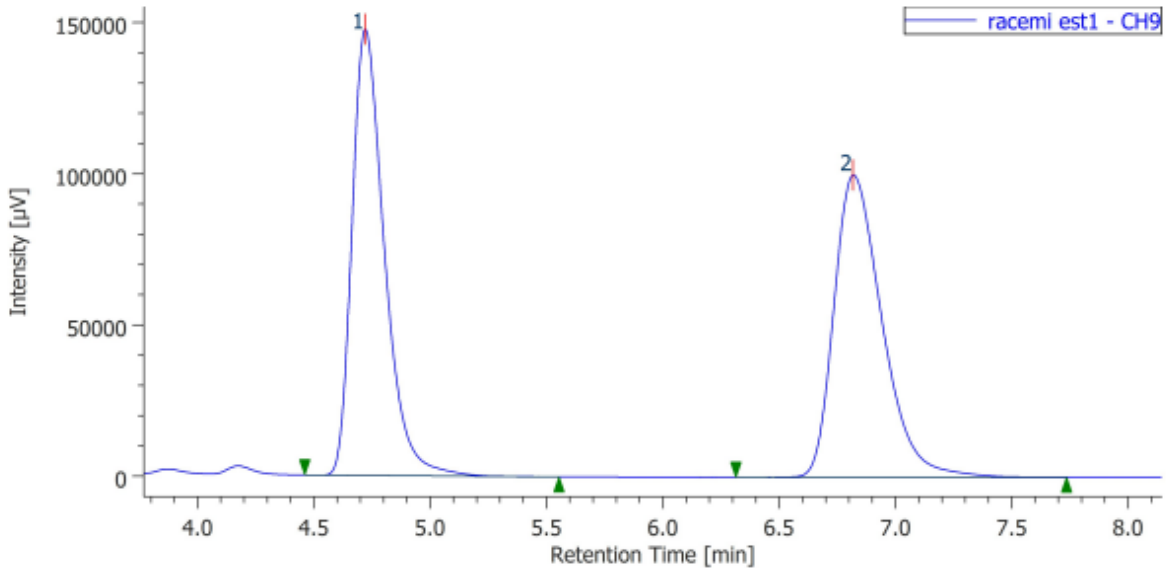
6-Fluoro-1-methyl-1,2,3,4-tetrahydronaphthalen-1-yl hexanoate (4d)

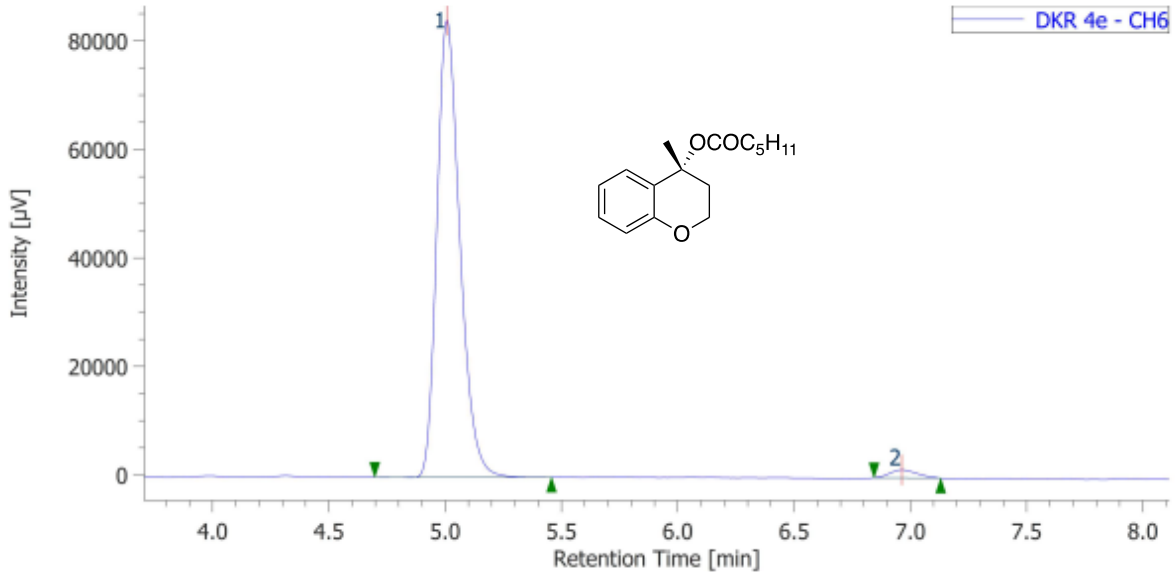




#	Peak Name	CH	tR [min]	Area [μV·sec]	Height [μV]	Area%	Height%	Quantity	NTP	Resolution	Symmetry Factor	Warning
1	Unknown	6	36.813	4868	51	0.235	0.133	N/A	451	1.428	85.989	
2	Unknown	6	42.733	2068180	38319	99.765	99.867	N/A	15392	N/A	1.329	

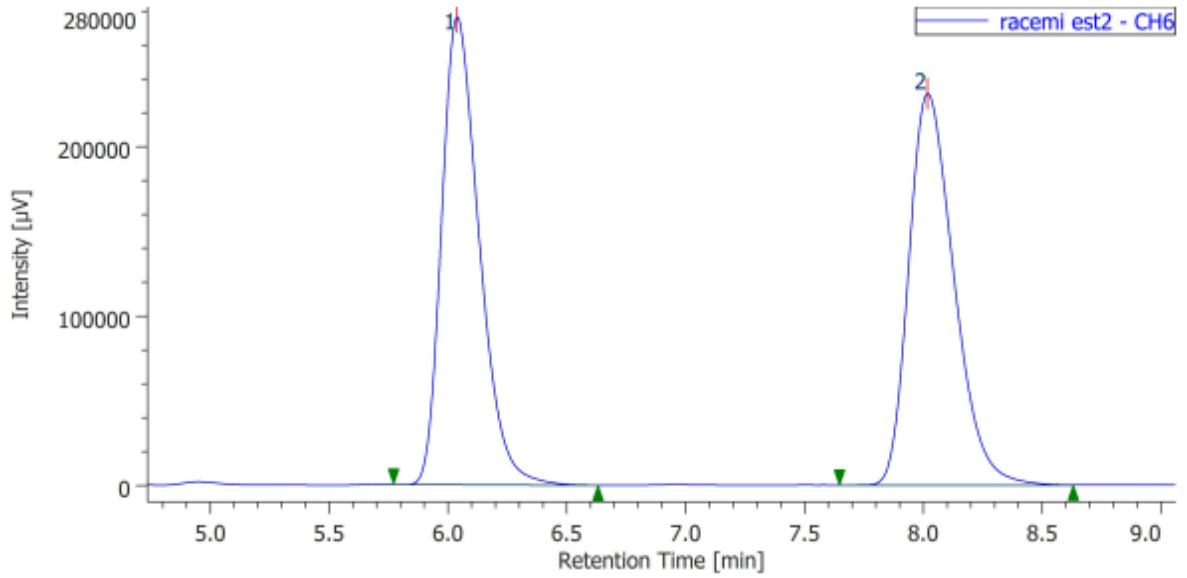
4-Methylchroman-4-yl hexanoate (4e)

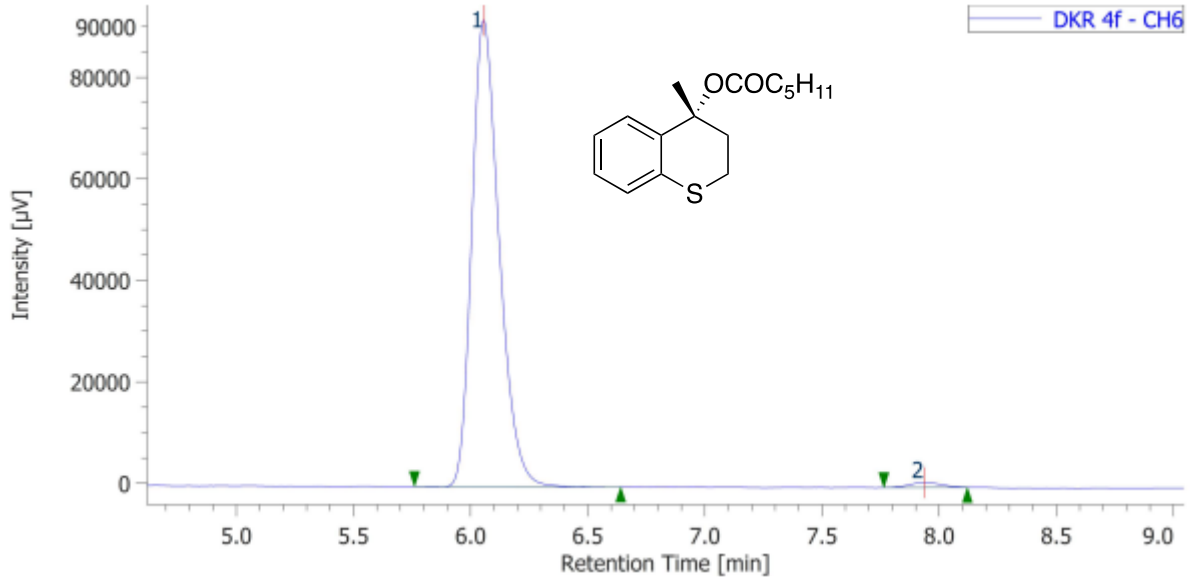




#	Peak Name	CH	tR [min]	Area [μV·sec]	Height [μV]	Area%	Height%	Quantity	NTP	Resolution	Symmetry Factor	Warning
1	Unknown	6	5.007	578279	84251	97.950	98.265	N/A	12704	9.850	1.292	
2	Unknown	6	6.963	12101	1487	2.050	1.735	N/A	15931	N/A	1.205	

4-Methylthiochroman-4-yl hexanoate (4f)





#	Peak Name	CH	tR [min]	Area [μV·sec]	Height [μV]	Area%	Height%	Quantity	NTP	Resolution	Symmetry Factor	Warning
1	Unknown	6	6.057	746354	91840	98.776	98.946	N/A	13264	8.069	1.275	
2	Unknown	6	7.937	9252	978	1.224	1.054	N/A	15276	N/A	1.084	